GEOS 22060/ GEOS 32060 / ASTR 45900

What makes a planet habitable?

Ice covered oceans, concluded → Exoplanets

Lecture 17

Thursday 30 May 2019

Ice-covered oceans

Persistent global ice cover:

DATA

PHYSICAL BASIS FOR LONG-TERM OCEAN STABILITY

ENERGETIC CONSTRAINTS ON BIOSPHERES

FUTURE TESTS AND TECHNIQUES

Energy budget of Europa's ocean

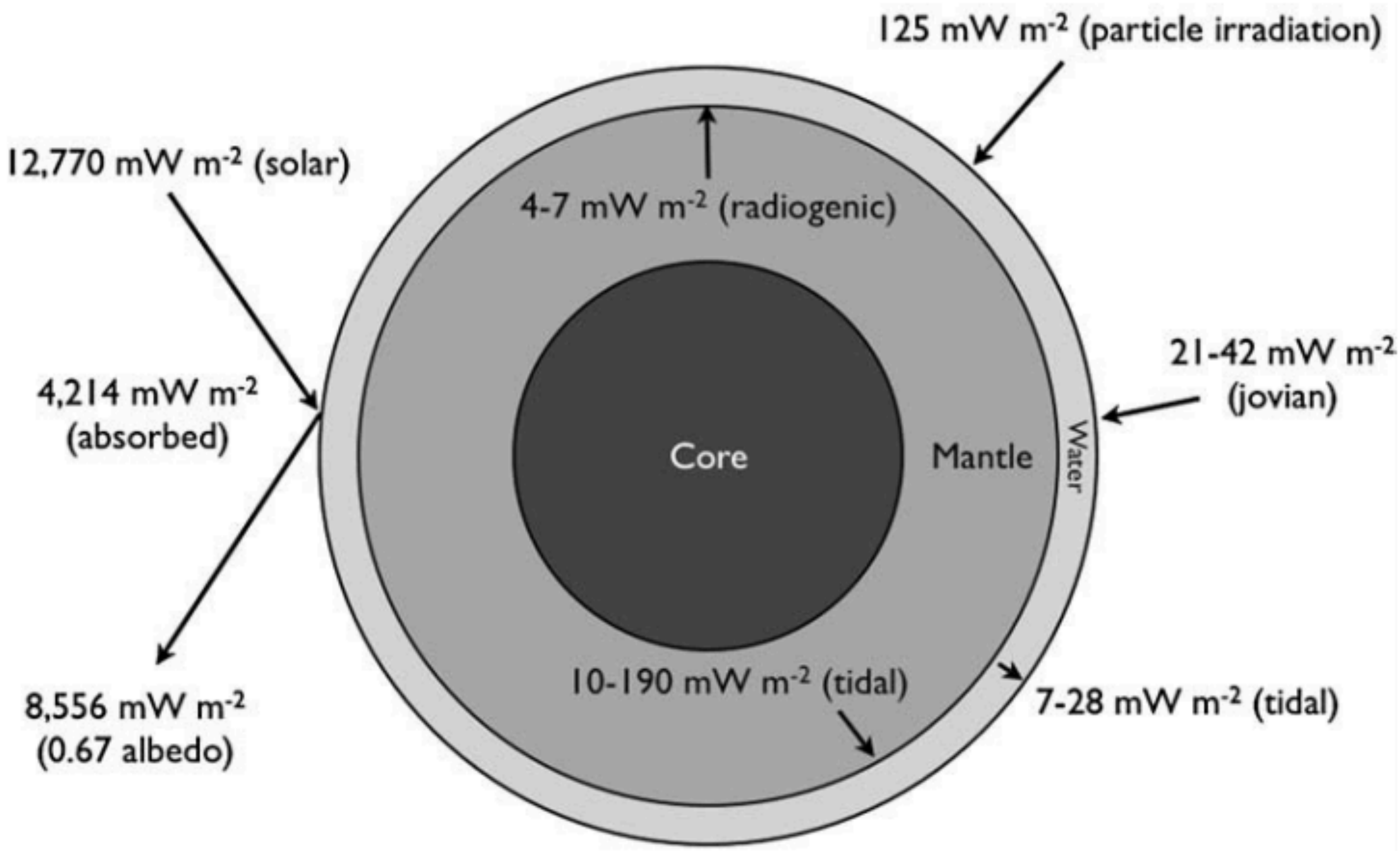

Hand et al. 2007

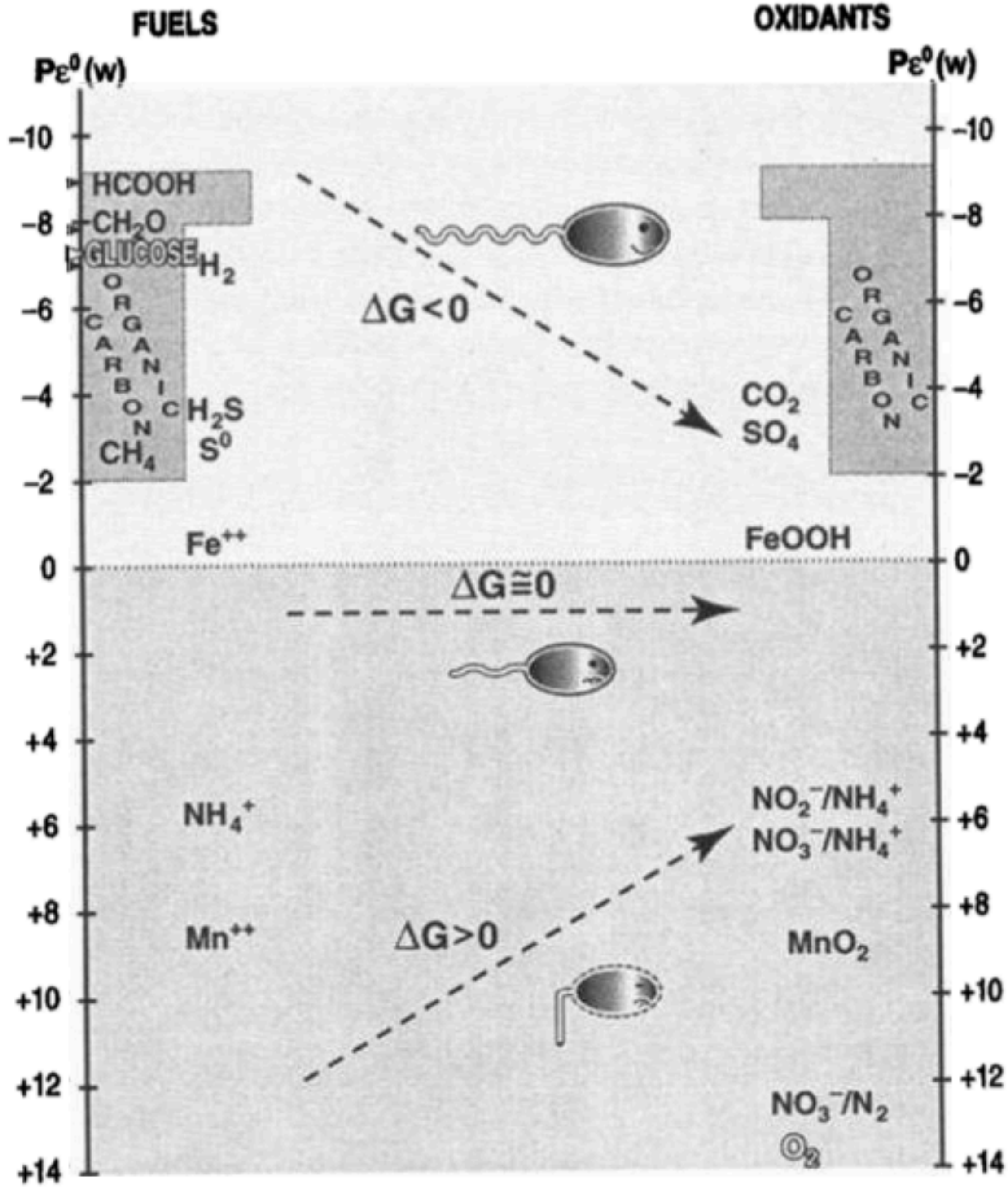

Thermodynamics: The Chemical Fuels and Oxidants of Life

K. Nealson
JGR Planets
1997

Giant-planet magnetic fields entrain charged particles which bombard the trailing hemispheres of moons → radiolytic chemistry

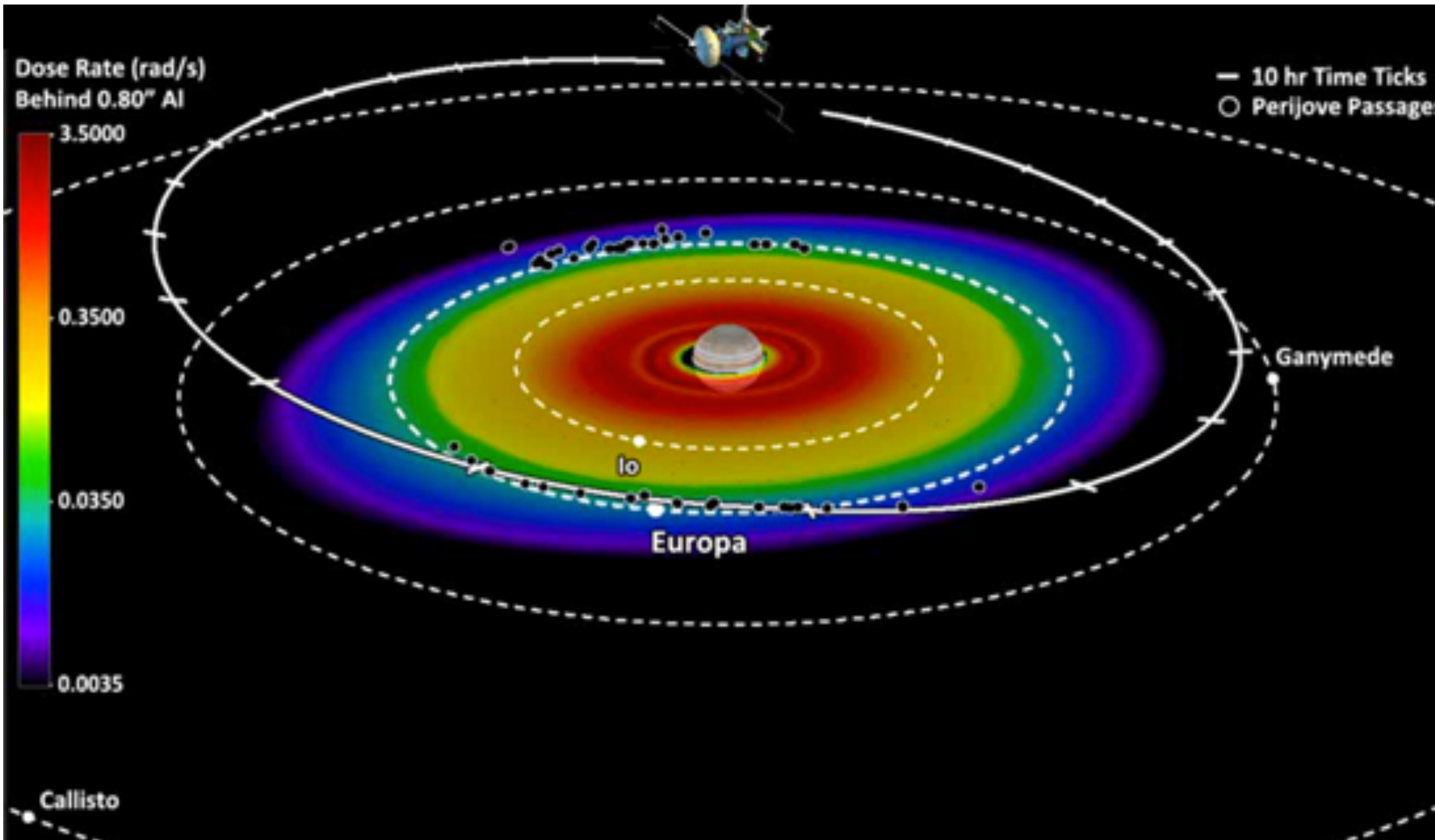

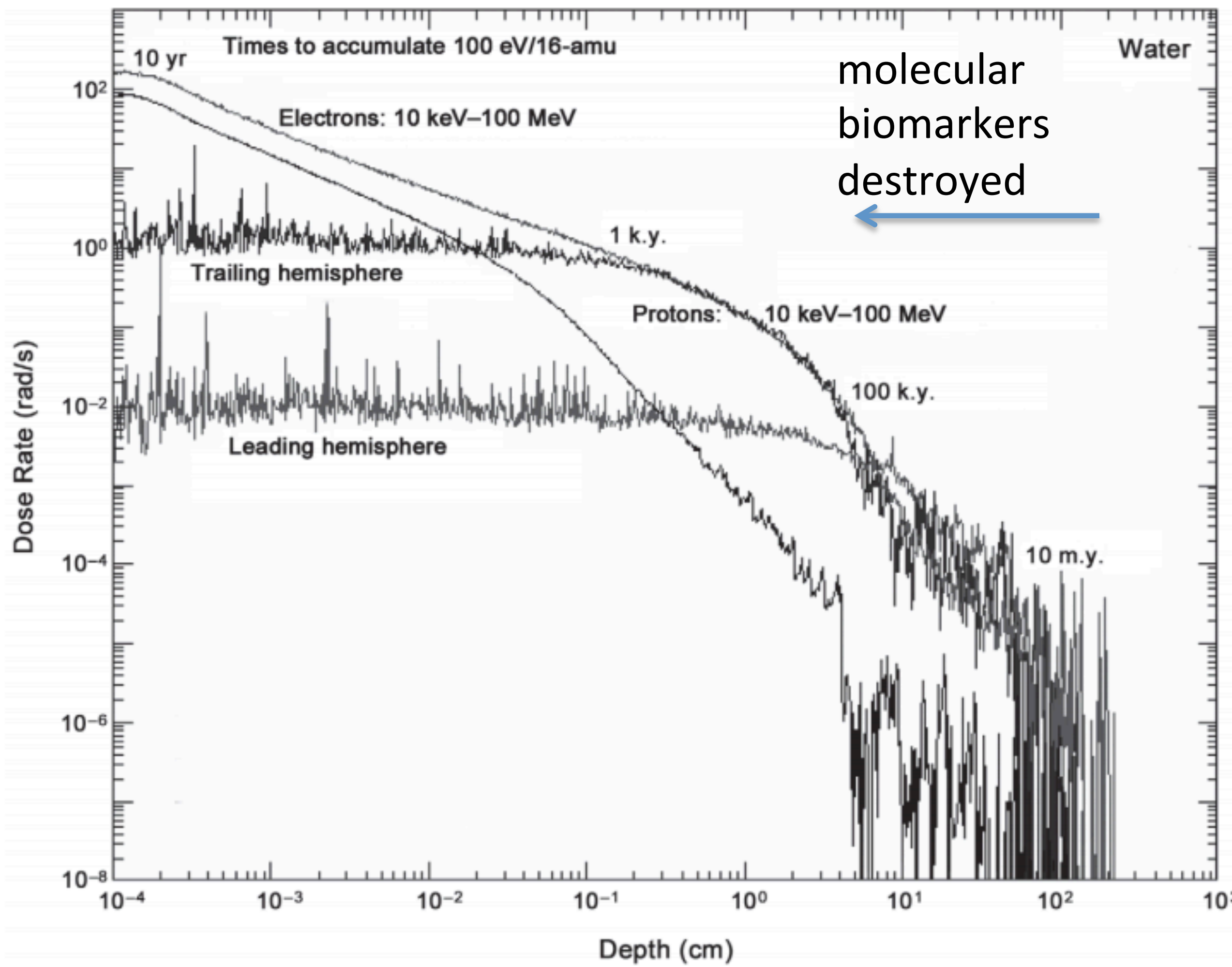

Fig. 10. After *Cooper and Sturner* (2006). Dose rate vs. depth where 1 rad/s is equal to 100 erg/gm/s or about 0.06 eV/H_2O-molecule/yr. The curve labeled "trailing hemisphere" includes the dose rate of 1–20-MeV electrons only, whereas the curve below it labeled leading hemisphere displays the dose rate of 20–40-MeV electrons that drift opposite to corotation. The uppermost of all the curves is the dose rate corresponding to electrons from 10 keV to 100 MeV and the dose rate from protons between 10 keV and 100 MeV follows this curve below it. Spikes and fluctuations in the computed curves arise from statistics of limited number of Monte Carlo events used in the simulations and not from physical processes. Times in years are shown to give chemically significant (most bonds are broken at least once) dose of 100-eV/16-amu (60 Gigarads) at selected dose levels.

from Paranicas et al., in the Europa Book, U. Arizona Press, 2009

An oxygen-rich Europa ocean, supplied by recycling of radiolytically-processed material from the surface?

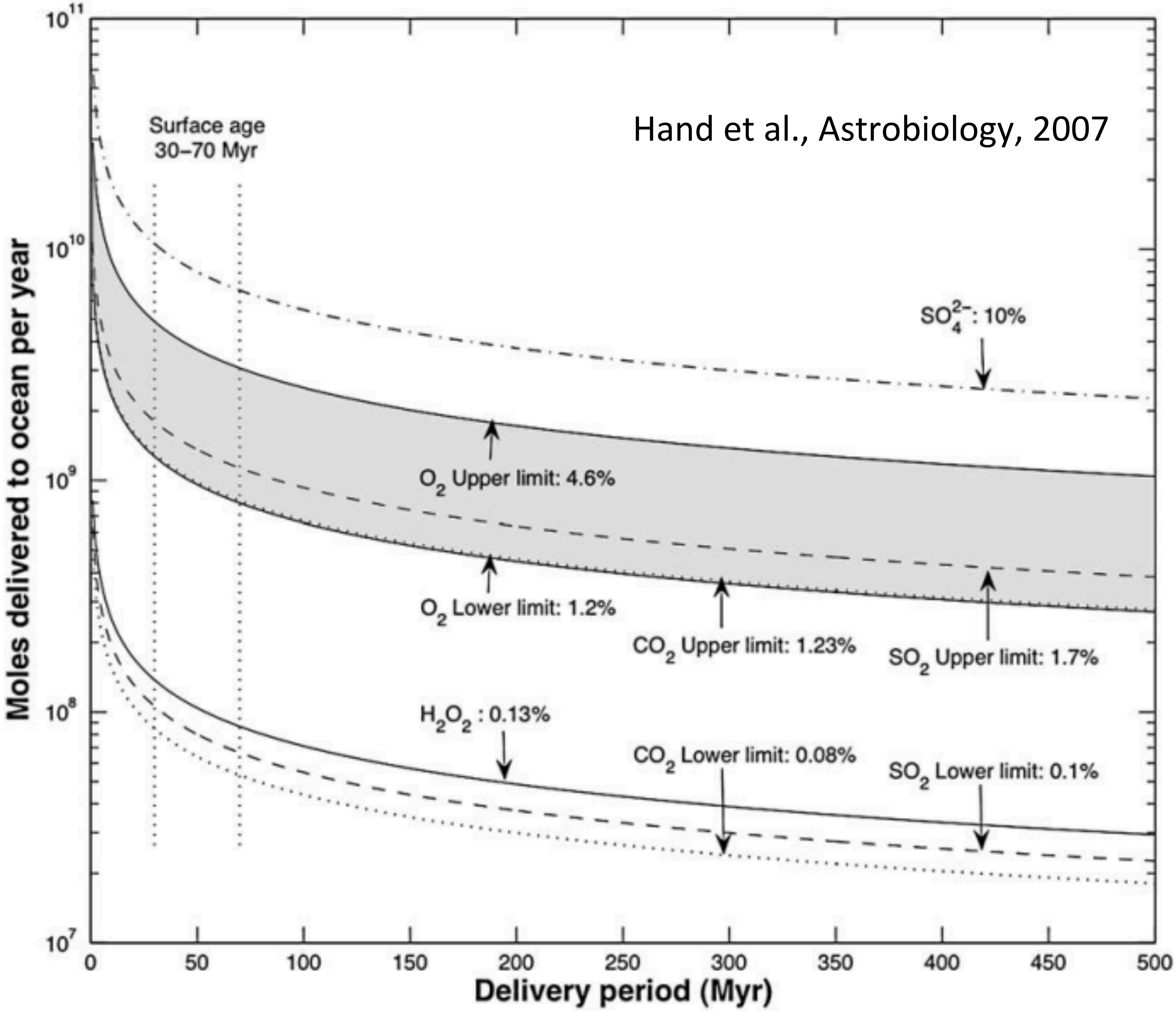

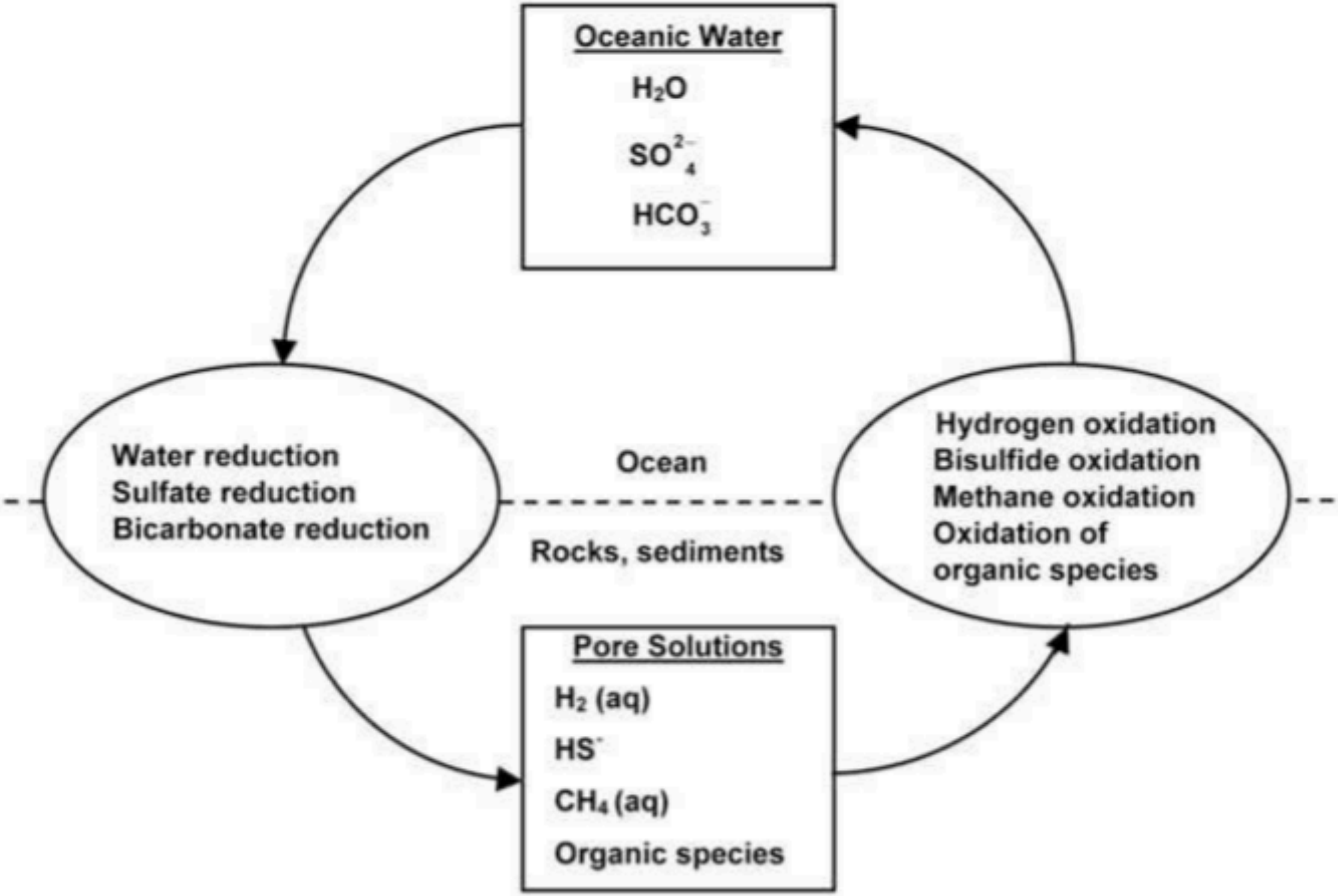
Oceanic Water
H_2O
SO_4^{2-}
HCO_3^-
Water reduction
Sulfate reduction
Bicarbonate reduction
Ocean
Rocks, sediments
Hydrogen oxidation
Bisulfide oxidation
Methane oxidation
Oxidation of organic species
Pore Solutions
H_2 (aq)
HS^-
CH_4 (aq)
Organic species

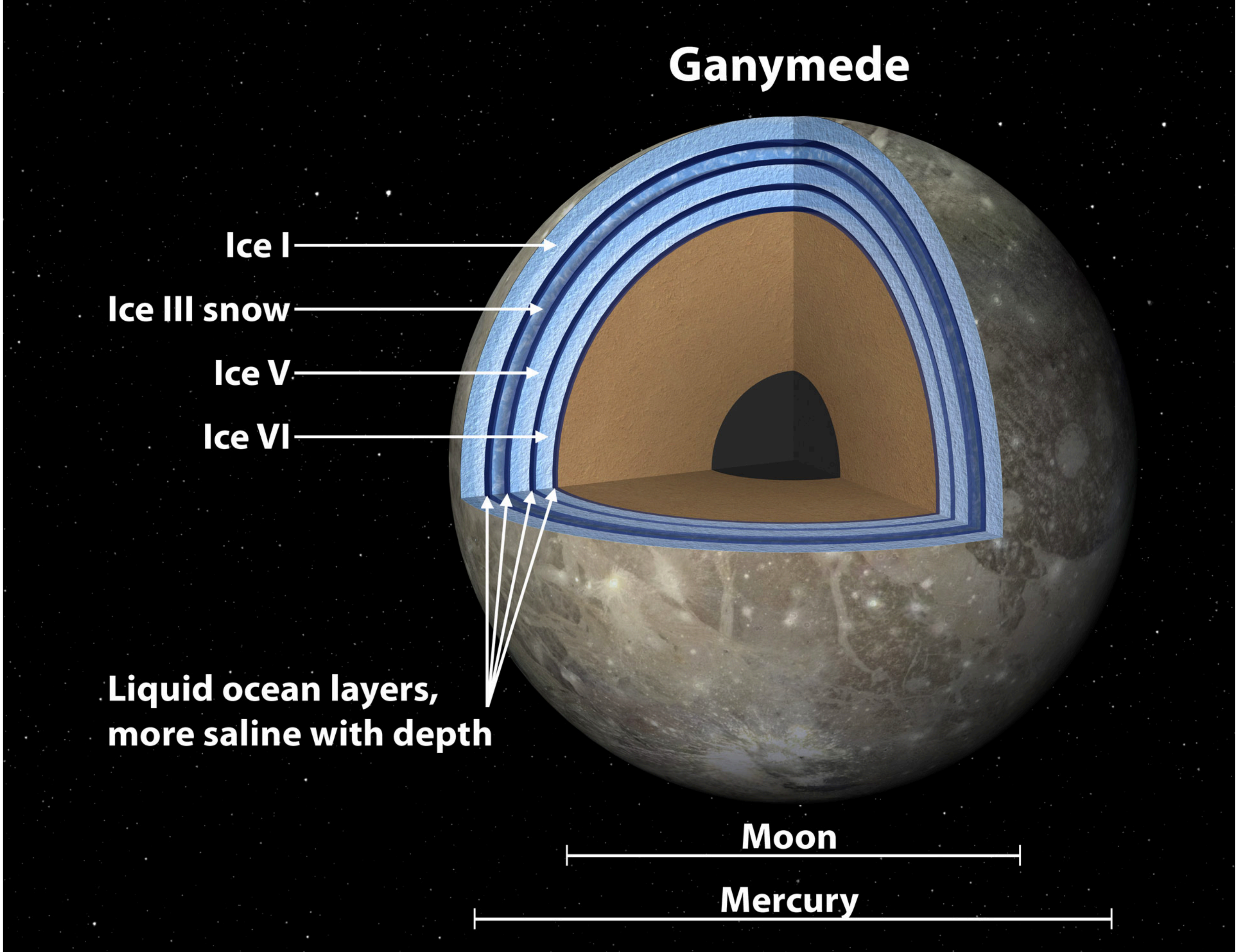
Ganymede
Ice I
Ice III snow
Ice V
Ice VI
Liquid ocean layers,
more saline with depth
Moon
Mercury

Ice-covered oceans

Persistent global ice cover:

DATA

PHYSICAL BASIS FOR LONG-TERM OCEAN STABILITY

ENERGETIC CONSTRAINTS ON BIOSPHERES

FUTURE TESTS AND TECHNIQUES

How to confirm a global sub-ice ocean exists: decoupling of ice shell from deep interior by ocean increases the amplitude of gravity tides and/or physical libration

Sciencexpress

The Tides of Titan

Luciano Iess,[1]* Robert A. Jacobson,[2] Marco Ducci,[1] David J. Stevenson,[3] Jonathan I. Lunine,[4] John W. Armstrong,[2] Sami W. Asmar,[2] Paolo Racioppa,[1] Nicole J. Rappaport,[2] Paolo Tortora[5]

[1]Dipartimento di Ingegneria Meccanica e Aerospaziale, Università La Sapienza, via Eudossiana 18, 00184 Rome, Italy. [2]Jet Propulsion Laboratory, 4800 Oak Grove Drive, Pasadena, CA 91109, USA. [3]California Institute of Technology, 150-21 Pasadena, CA 91125, USA. [4]Department of Astronomy, Cornell University, Ithaca, NY 14850, USA. [5]DIEM-II Facoltà di Ingegneria, Università di Bologna, I-47121 Forlì, Italy.

*To whom correspondence should be addressed. E-mail: luciano.iess@uniroma1.it

We have detected in Cassini data the signature of the periodic tidal stresses within Titan driven by the eccentricity (e = 0.028) of its 16-day orbit around Saturn. Precise measurements of the acceleration of the Cassini spacecraft during six close flybys between 2006 and 2011 have revealed that Titan responds to the variable tidal field exerted by Saturn with periodic changes of its quadrupole gravity, at about 4% of the static value. Two independent determinations of the corresponding degree-2 Love number yield $k_2 = 0.589 \pm 0.150$ and $k_2 = 0.637 \pm 0.224$ (2σ). Such a large response to the tidal field requires that Titan's interior is deformable over time scales of the orbital period, in a way that is consistent with a global ocean at depth.

Thomas et al. Icarus 2016

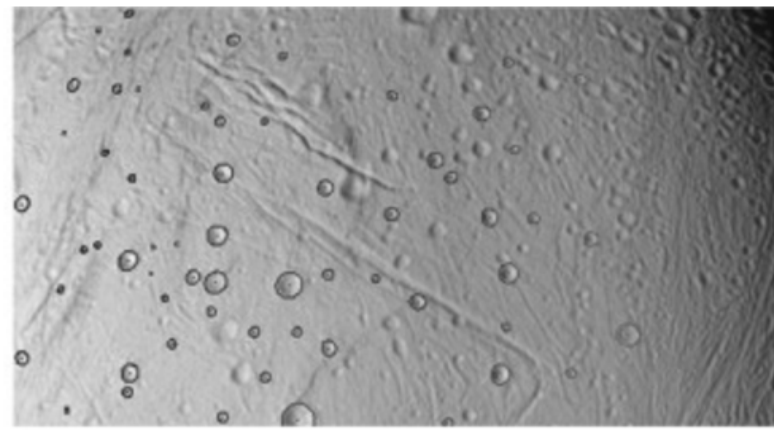

Measuring the thickness of the ice shell

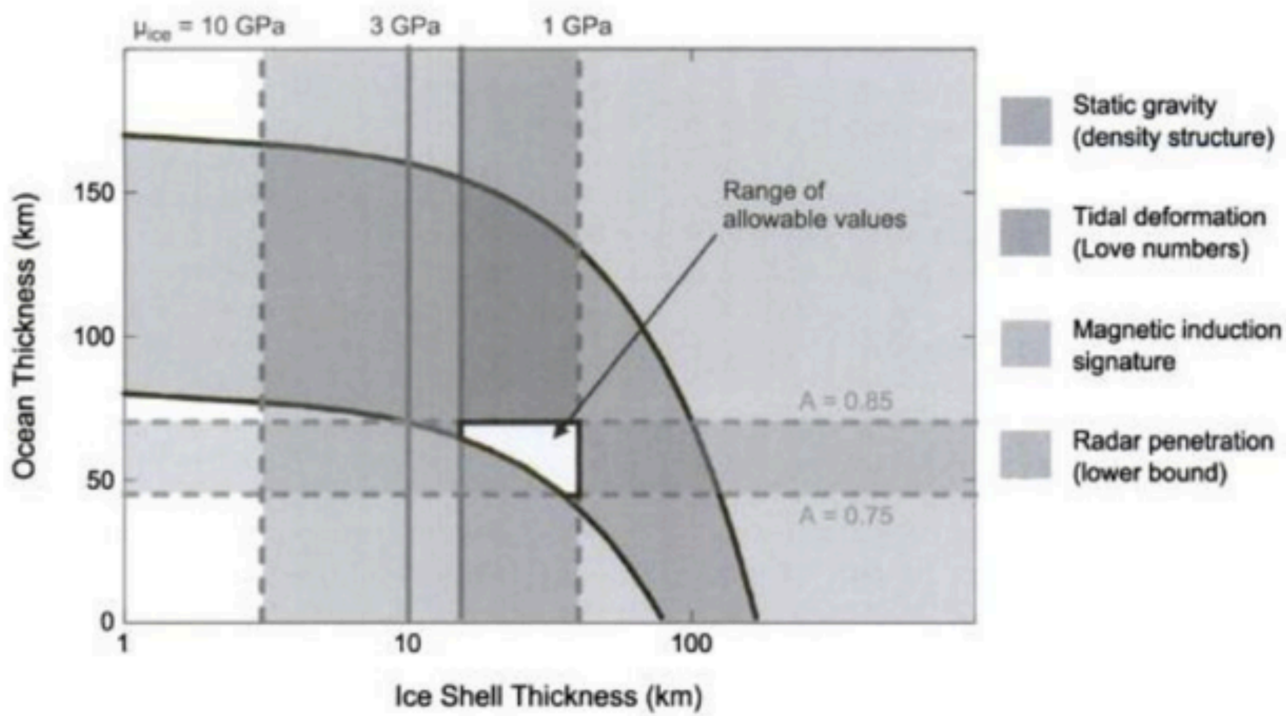

Fig. 7. See Plate 38. The combination of (hypothetical) JEO measurements can constrain the thickness of the icy shell. Based on the bulk density and moment of inertia (from future flybys by JEO and other spacecraft), the thickness of the water + ice layer may be obtained (gray shading) (*Anderson et al.*, 1998a,b); uncertainties arise mainly from lack of knowledge of the rocky interior density (bulk density is already known). Measuring time-variable gravity and topography gives the k_2 and h_2 Love numbers, respectively; hypothetical Love number constraints (red shading) assume observed h_2 and k_2 of 1.202 and 0.245, respectively, and constrain shell thickness as a function of rigidity μ (*Moore and Schubert*, 2000). The hypothetical values assumed here are characteristics of a moderately thick icy shell. In the example shown, the icy shell deformation is sufficiently large that a shell thickness in excess of 40 km is prohibited. Determining both k_2 and h_2 provides additional information. A lower bound on the icy shell thicknesses may be derived from radar data. Here, a tectonic model of icy shell properties is assumed (*Moore*, 2000), resulting in a radar penetration depth (and lower bound on shell thickness) of 15 km (green shading). Multiple frequency (hypothetical) set of observations results in a range of acceptable icy shell thickness (15–40 km) and a range of acceptable ocean thicknesses (45–70 km). A different set of observations would result in different constraints, but the combined constraints are more rigorous than could be achieved by any one technique alone. JEO would be able to provide those constraints to determine the thickness of Europa's icy shell.

Landing and recovering ocean materials

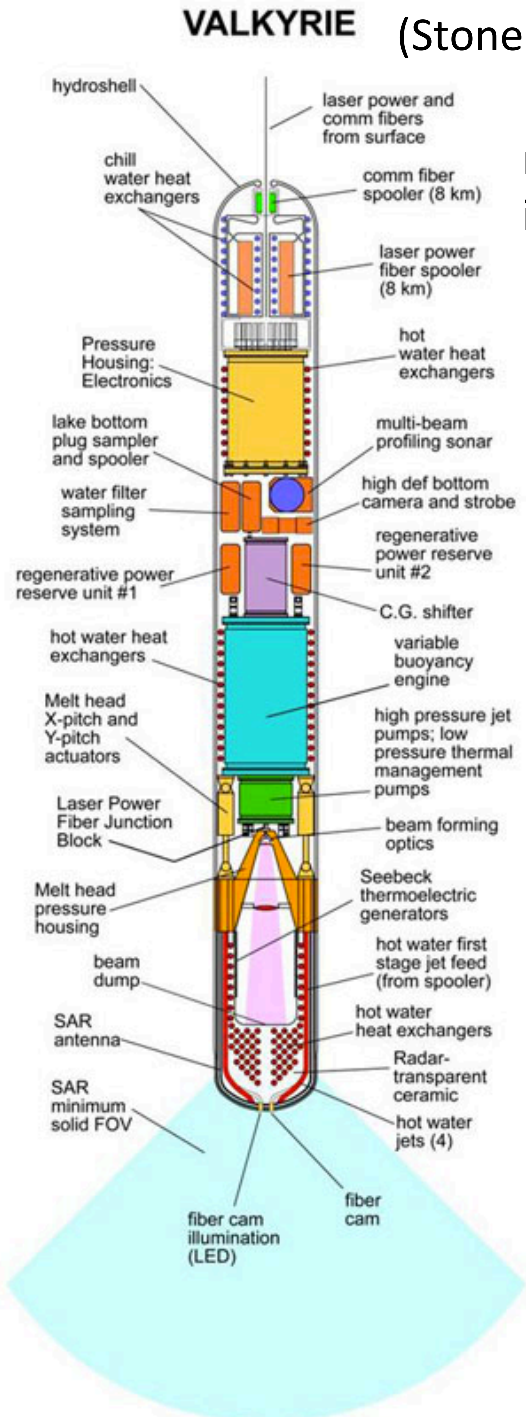

(Stone Aerospace)

nuclear reactor is required

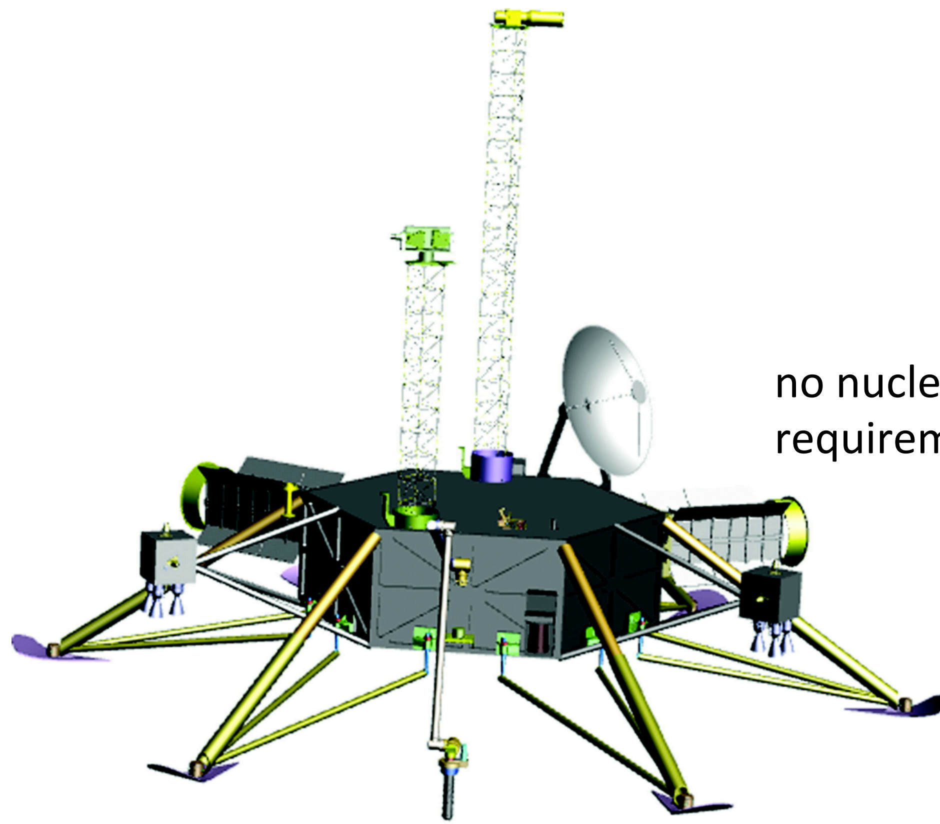

no nuclear reactor requirement

A shortcut: sample material from the cryovolcanic plumes of Saturn's moon Enceladus

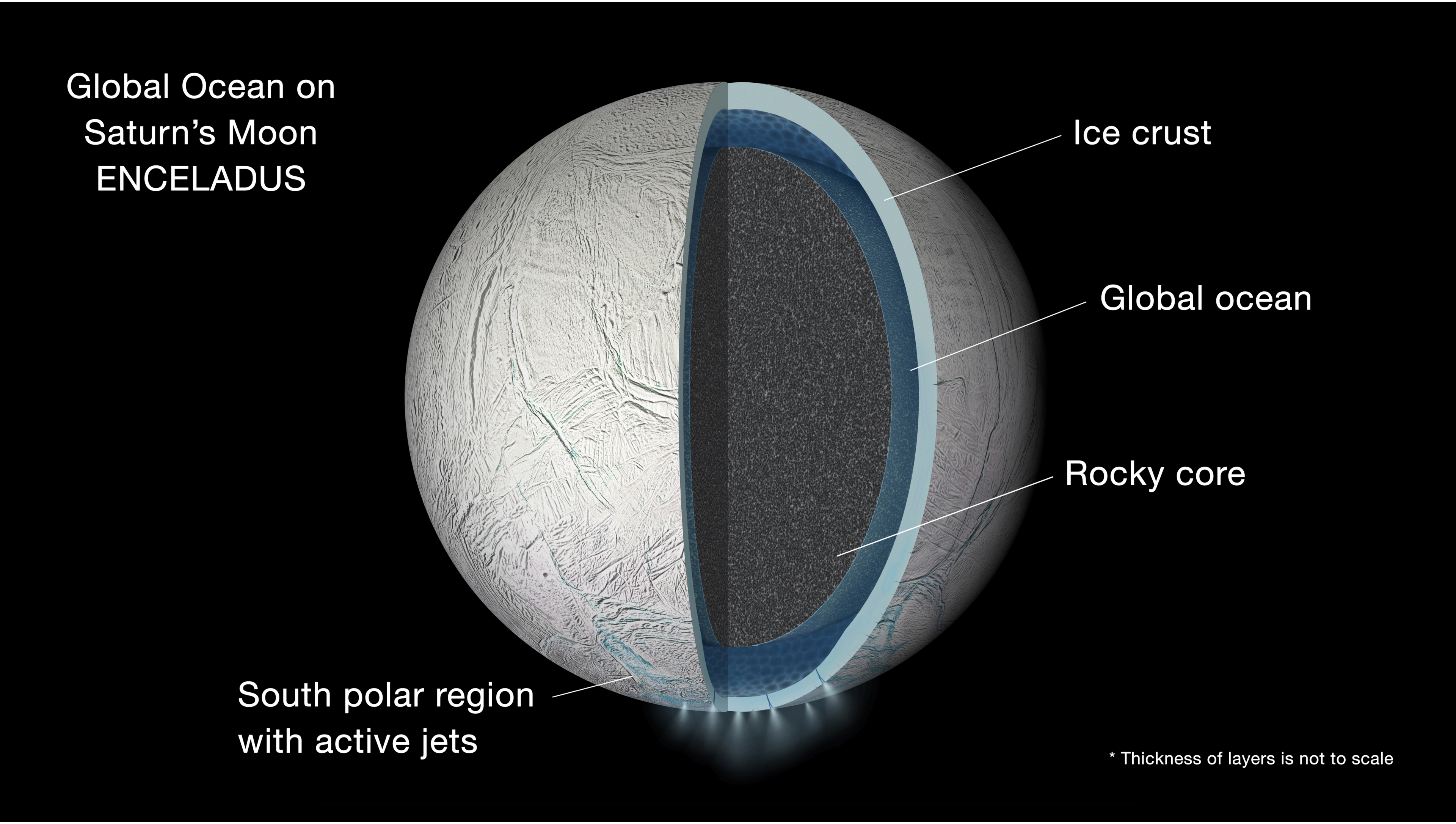

NASA/JPL

The ‘tiger stripes’ that launch Enceladus’ geysers are gateways to a global ocean

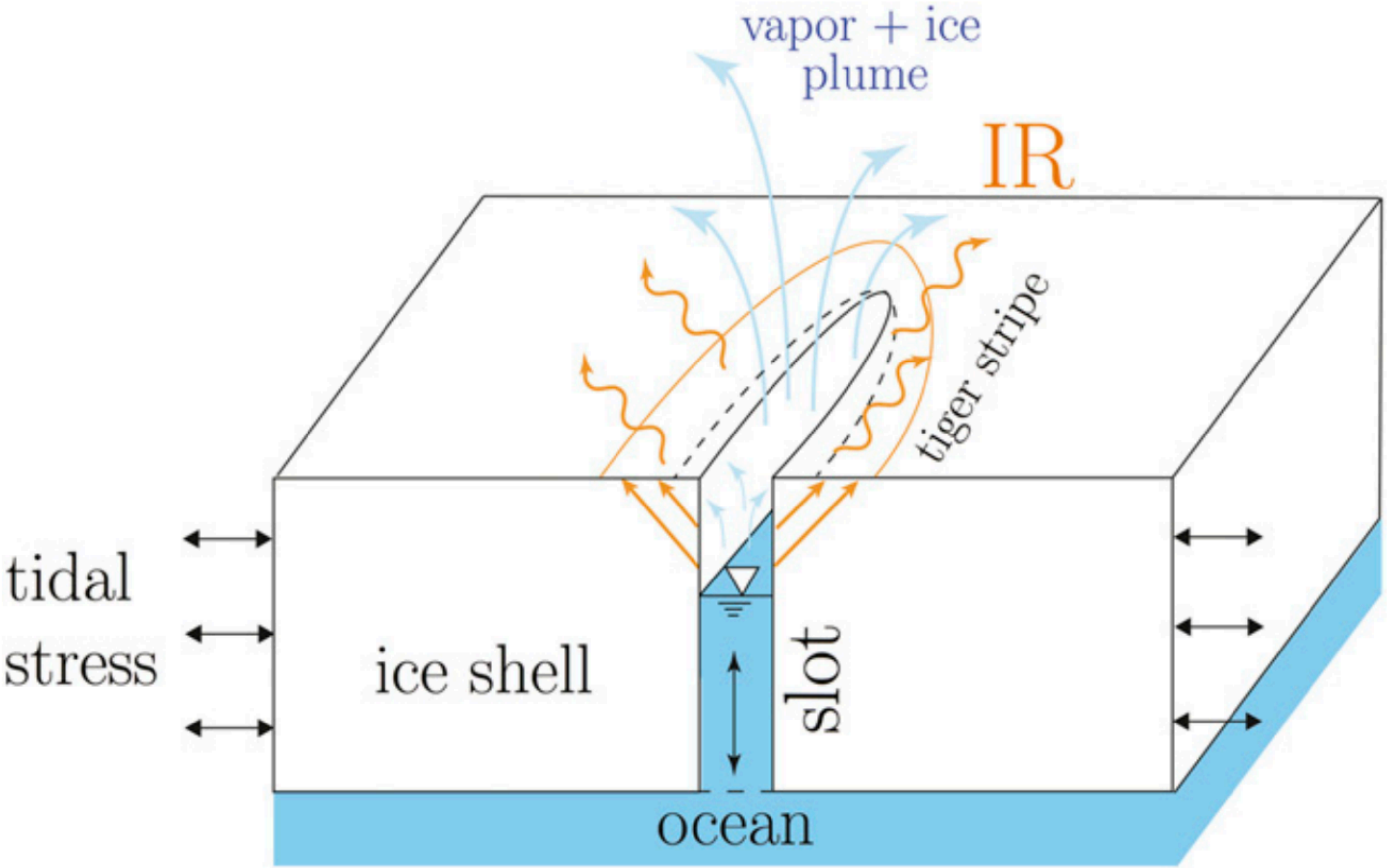

Fig. 1. The erupted flux from Enceladus (blue arrows) varies on diurnal timescales, which we attribute to daily flexing (dashed lines) of the source fissures by Saturn tidal stresses (horizontal arrows). Such flexing would also drive vertical flow in slots underneath the source fissures (vertical black arrow), which through viscous dissipation generates heat. This heat helps to maintain the slots against freezeout despite strong evaporitic cooling by vapor escaping from the water table (downward-pointing triangle). The vapor ultimately provides heat (via condensation) for the envelope of warm surface material bracketing the tiger stripes (orange arrows; “IR” corresponds to infrared cooling from this warm material).

Kite & Rubin PNAS 2016

Hydrothermal vents were active at the Enceladus seafloor geologically recently (inference: probably active today also)

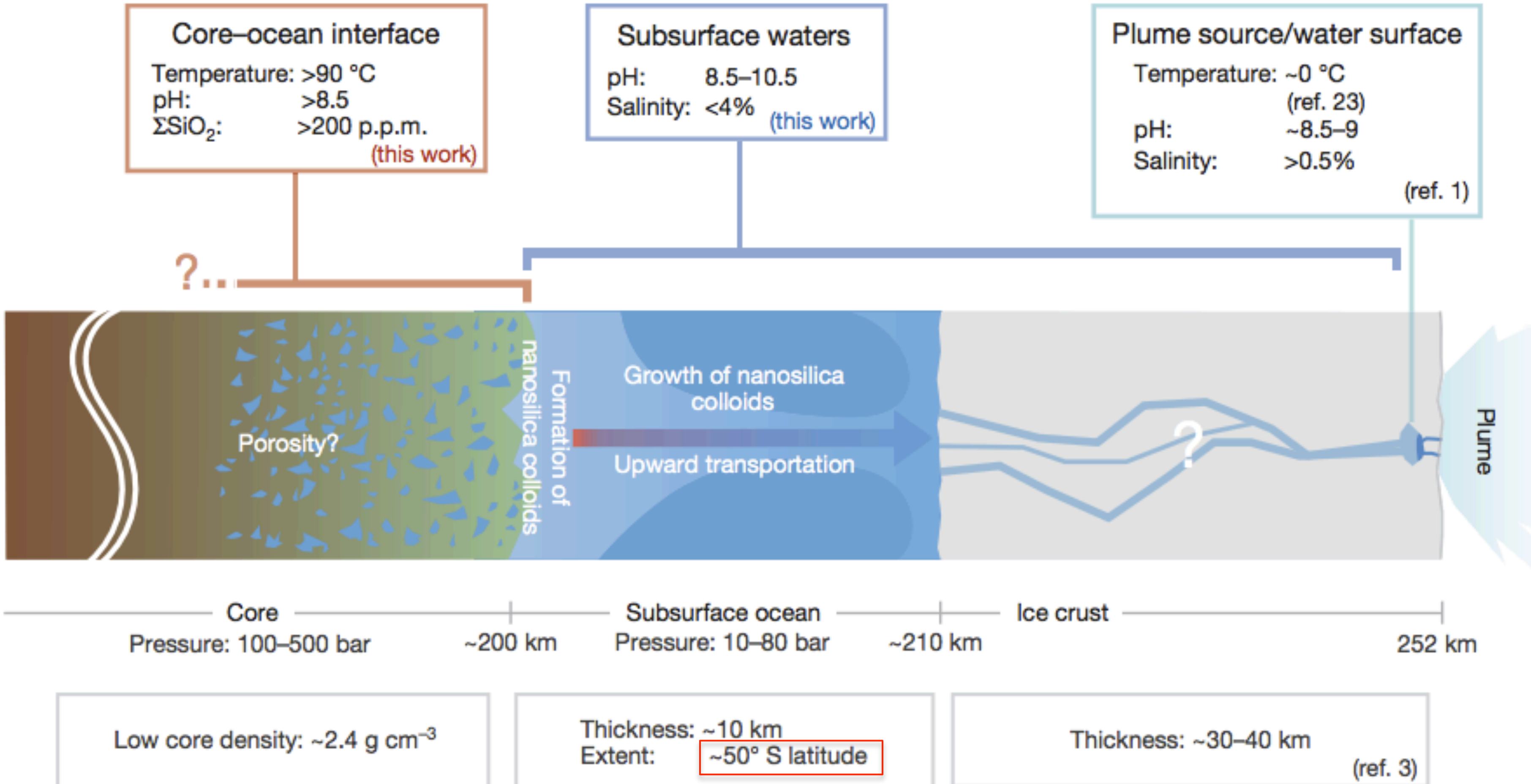

not correct – now known to be global

Hsu et al. Nature 2015

Energy is available for life on Enceladus

$$CO_2(aq) + 4H_2(aq) \rightarrow CH_4(aq) + 2H_2O(l)$$

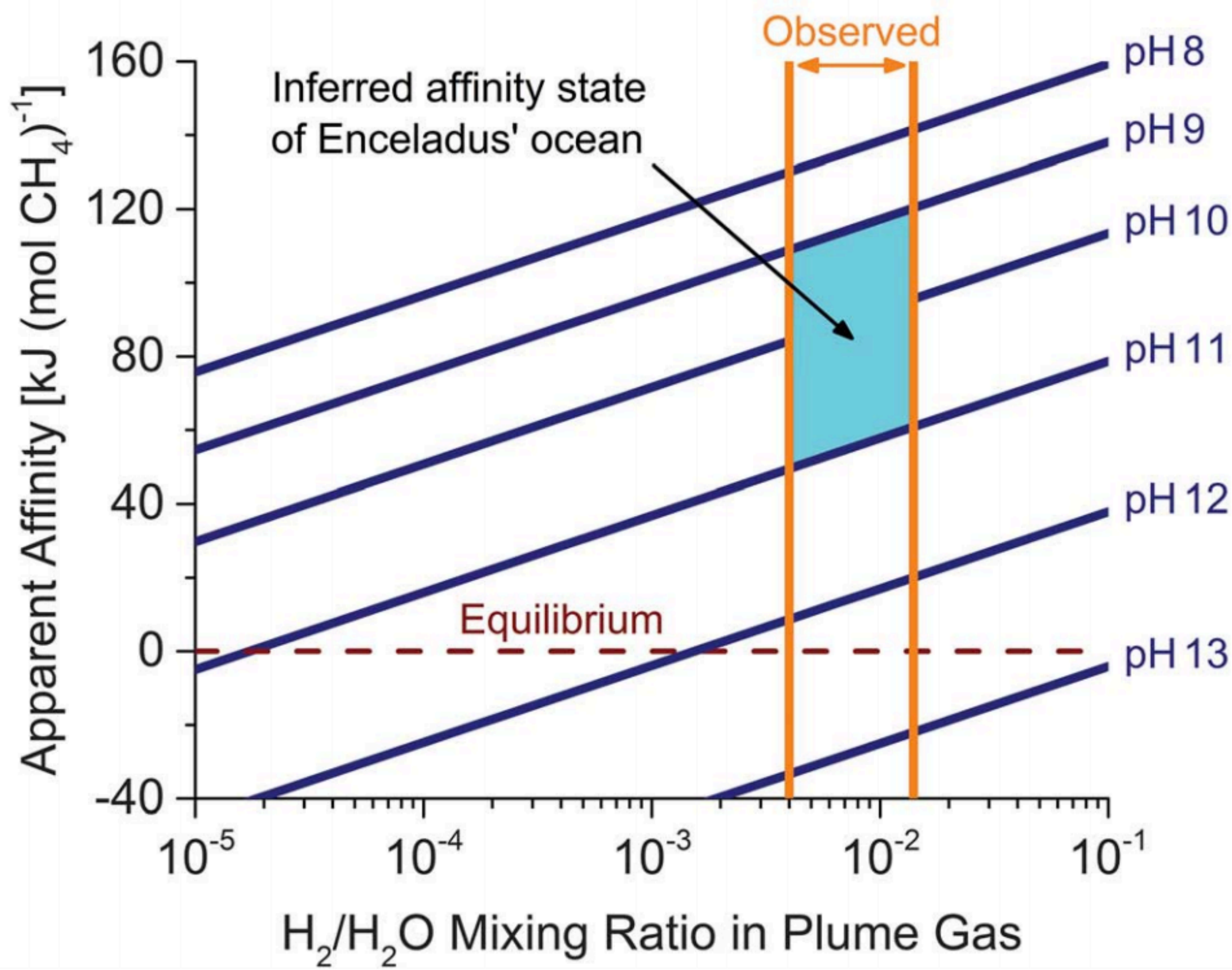

Fig. 4. Apparent chemical affinity for hydrogenotrophic methanogenesis in the ocean of Enceladus (273 K, 1 bar). The orange lines bracket the observed range in the mixing ratio of H_2 in the plume gas (Table 1). The dark blue lines are contours of constant ocean pH, a key model parameter. The cyan region indicates affinities for a pH range that may provide the greatest consistency between the results of (*13*, *15*, *25*). The dashed burgundy line designates chemical equilibrium, where no energy would be available from methanogenesis. These nominal model results are based on $CH_4/CO_2 = 0.4$ (Table 1), a chlorinity of 0.1 molal, and 0.03 molal total dissolved carbonate (*25*). Reported ranges in these parameters propagate to give an uncertainty in the computed affinities of ~10 kJ (mol CH_4)$^{-1}$.

Waite et al. Nature 2017

Complex organic molecules are being launched into space from a scum layer on the top of Enceladus' ocean

Postberg et al Nature 2018

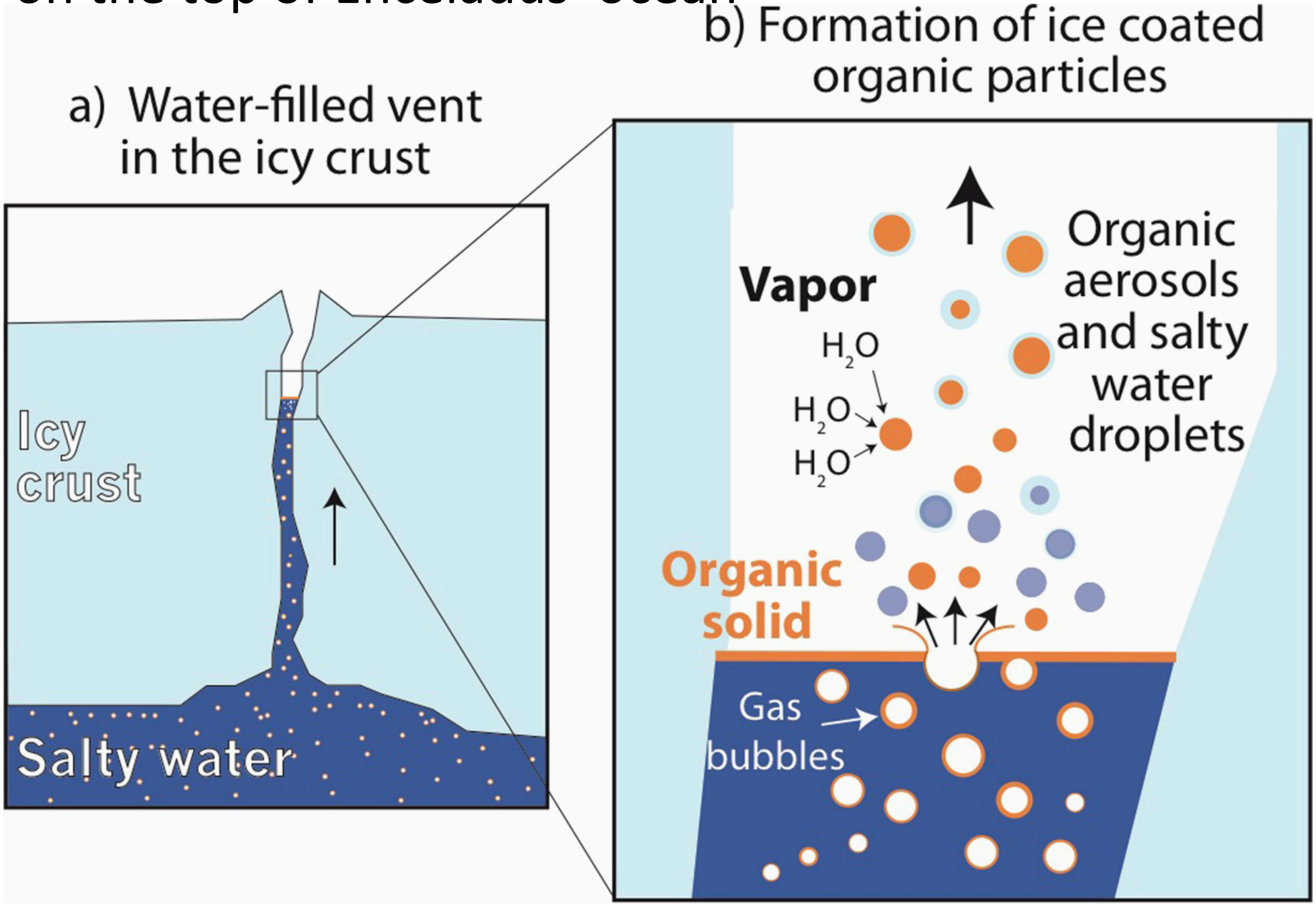

Extended Data Fig. 12 | Schematic on the formation of organic condensation cores from a refractory organic film. a, Ascending gas bubbles in the ocean[25] efficiently transport organic material[30] into water-filled cracks in the south polar ice crust. **b**, Organics ultimately concentrate in a thin organic layer (orange) on top of the water table, located inside the icy vents. When gas bubbles burst, they form aerosols made of insoluble organic material that later serve as efficient condensation cores for the production of an icy crust from water vapour, thereby forming HMOC-type particles. In parallel, larger, pure salt-water droplets form (blue), which freeze and are later detected by the CDA as salt-rich type-3 ice particles in the plume[8,9].

Key points from today's lecture

- evidence for global sub-ice oceans in the outer Solar System;
- the "ideal" sub-ice ocean for biology (and ways in which Europa, Ganymede and Enceladus deviate from that ideal).

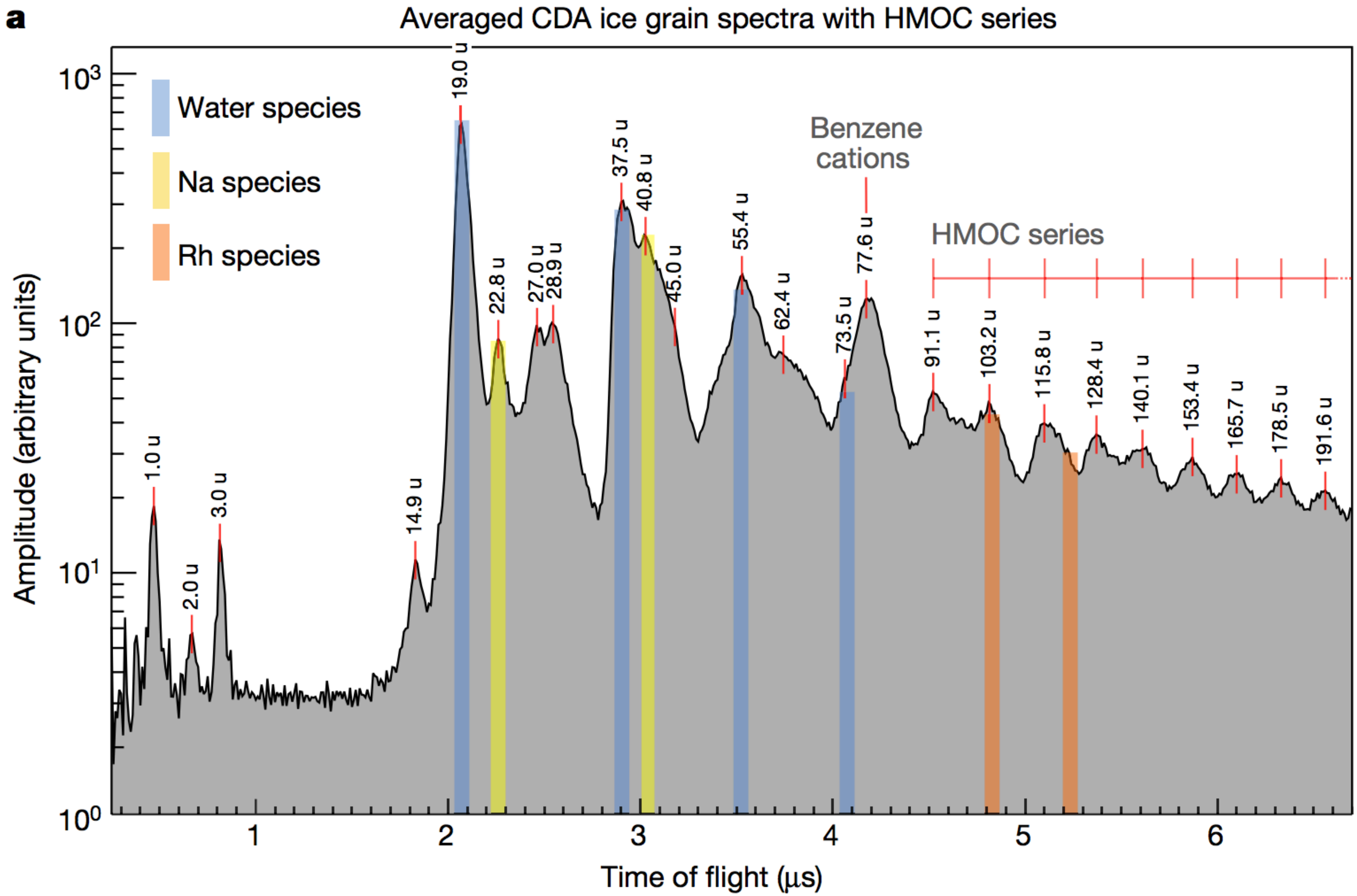

a
Averaged CDA ice grain spectra with HMOC series
Water species
Na species
Rh species
Benzene cations
HMOC series
1.0 u
2.0 u
3.0 u
14.9 u
19.0 u
22.8 u
27.0 u
28.9 u
37.5 u
40.8 u
45.0 u
55.4 u
62.4 u
73.5 u
77.6 u
91.1 u
103.2 u
115.8 u
128.4 u
140.1 u
153.4 u
165.7 u
178.5 u
191.6 u
Amplitude (arbitrary units)
10^3
10^2
10^1
10^0
Time of flight (μs)
1
2
3
4
5
6

Exoplanet habitability

HABITABLE-ZONE 1-2 EARTH RADIUS PLANETS ARE NUMEROUS

HABITABLE-ZONE 1-2 EARTH RADIUS PLANETS ARE LIKELY DIVERSE COMPOSITIONALLY

- MG/SI/FE
- WATER
- CARBON

THE M-STAR OPPORTUNITY

- PROBLEMS FOR HABITABILITY FOR PLANETS ORBITING M-STARS

INTERSTELLAR MISSIONS?

Exoplanets are detected mainly through radial velocity measurements and transits

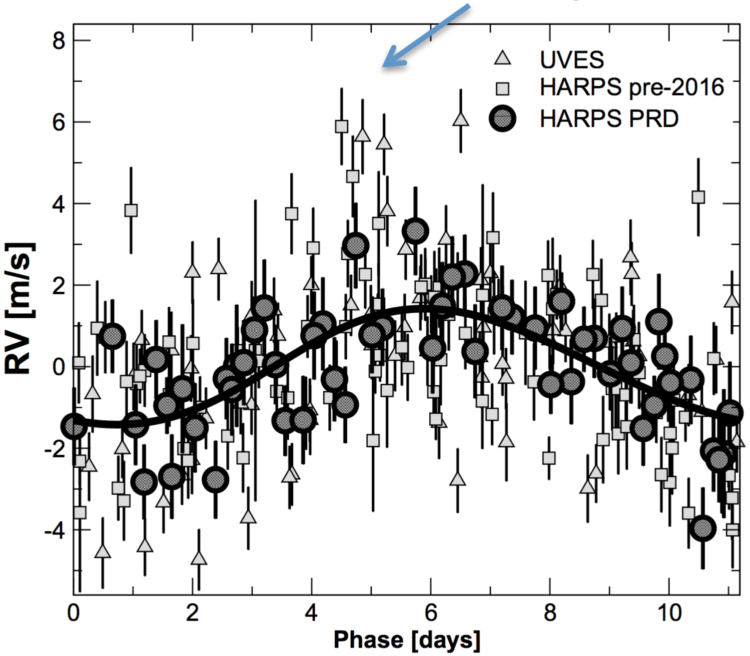

Proxima Centauri b
Anglada-Escudé et al. 2016

TRAPPIST-1 (Gillon et al. 2016)

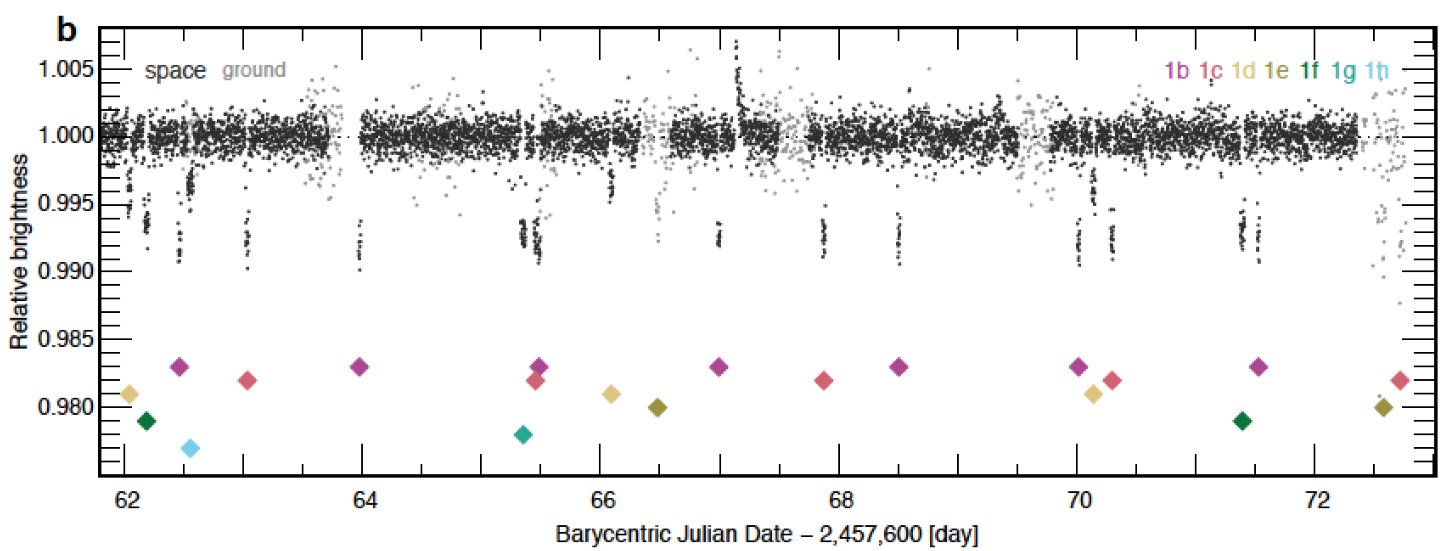

HABITABLE-ZONE 1-2 EARTH RADIUS PLANETS ARE NUMEROUS

Sunlike (FGK) stars:

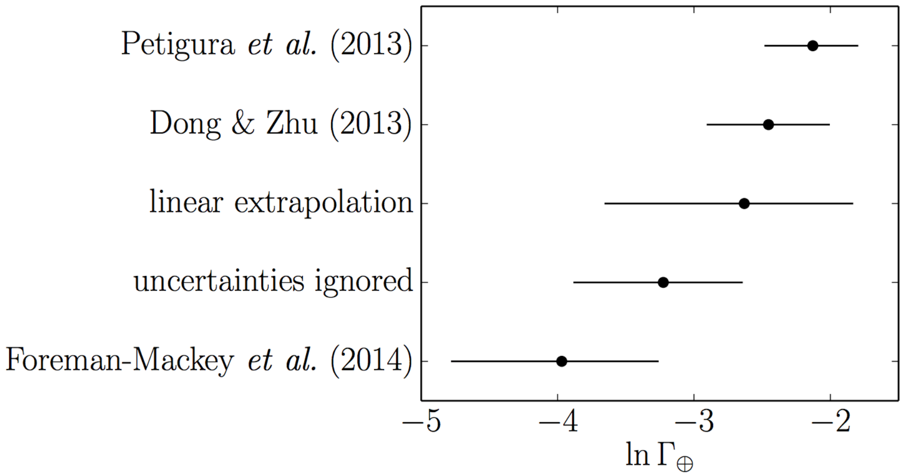

$$\Gamma_\oplus = \left.\frac{\mathrm{d}N}{\mathrm{d}\ln P\;\mathrm{d}\ln R}\right|_{R=R_\oplus,\,P=P_\oplus}$$

Red dwarf (M) stars:

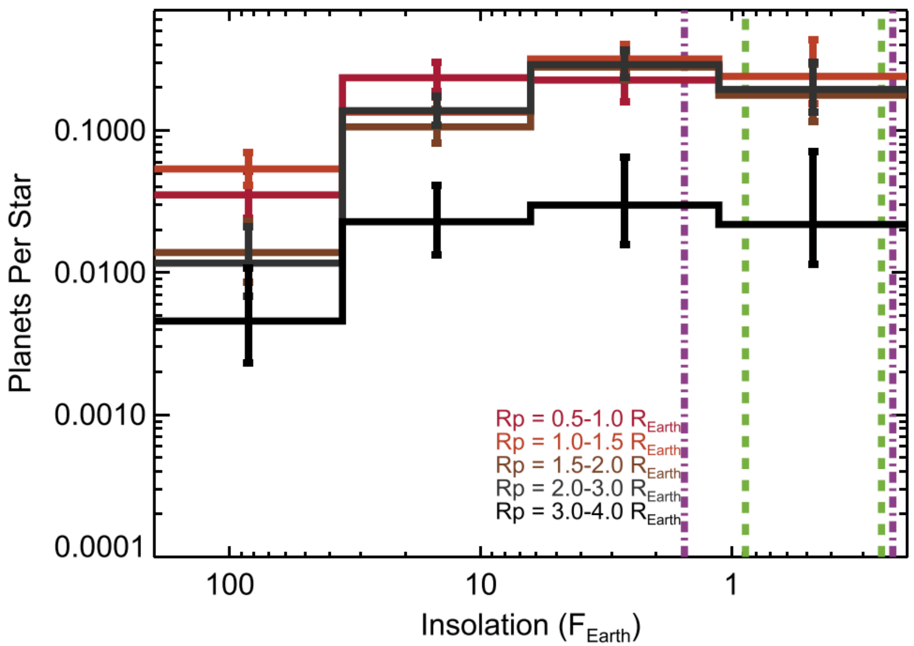

Dressing & Charbonneau ApJ 2015

HABITABLE-ZONE 1-2 EARTH RADIUS PLANETS ARE LIKELY DIVERSE COMPOSITIONALLY

- HYDROGEN
- MG/SI/FE
- WATER
- CARBON

HABITABLE-ZONE 1-2 EARTH RADIUS PLANETS ARE LIKELY DIVERSE COMPOSITIONALLY - HYDROGEN

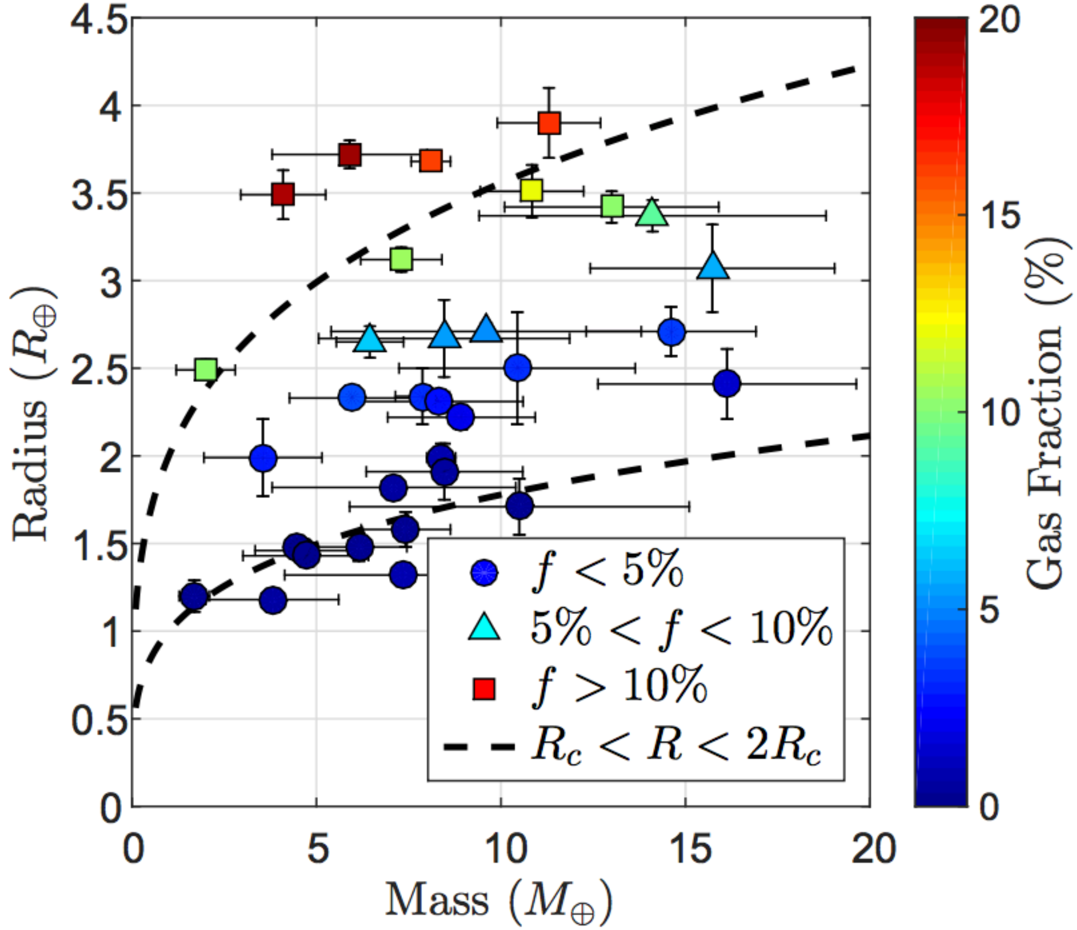

Ginzberg et al.
ApJ 2016

FIG. 2.— Observed super-Earth population (see text for details) from Weiss & Marcy (2014). The planets are grouped according to their gas mass fraction f, estimated by Equation (38), with low-density planets marked by triangles ($5\% < f < 10\%$) or squares ($f > 10\%$). The planet markers are also color-coded according to f. The two dashed black lines mark the radius of the rocky core $R_c(M_c)$ and $2R_c(M_c)$. Planets with substantial atmospheres are expected to be found roughly between the two lines.

HABITABLE-ZONE 1-2 EARTH RADIUS PLANETS ARE LIKELY DIVERSE COMPOSITIONALLY

- MG/SI, MG/FE, e.t.c.

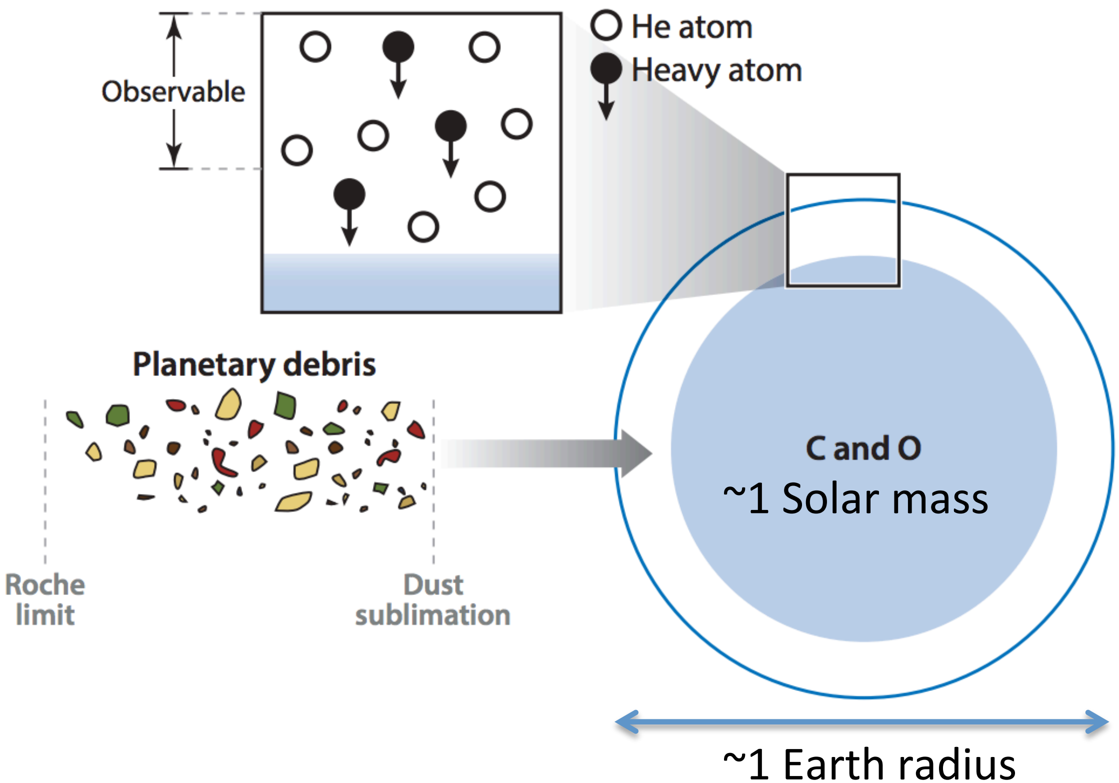

Constrained mainly by compositions of white dwarfs that are accreting material fderived from tidally shredded planets.

Jura & Young, 'Extrasolar cosmochemistry,' Annual Reviews, 2014

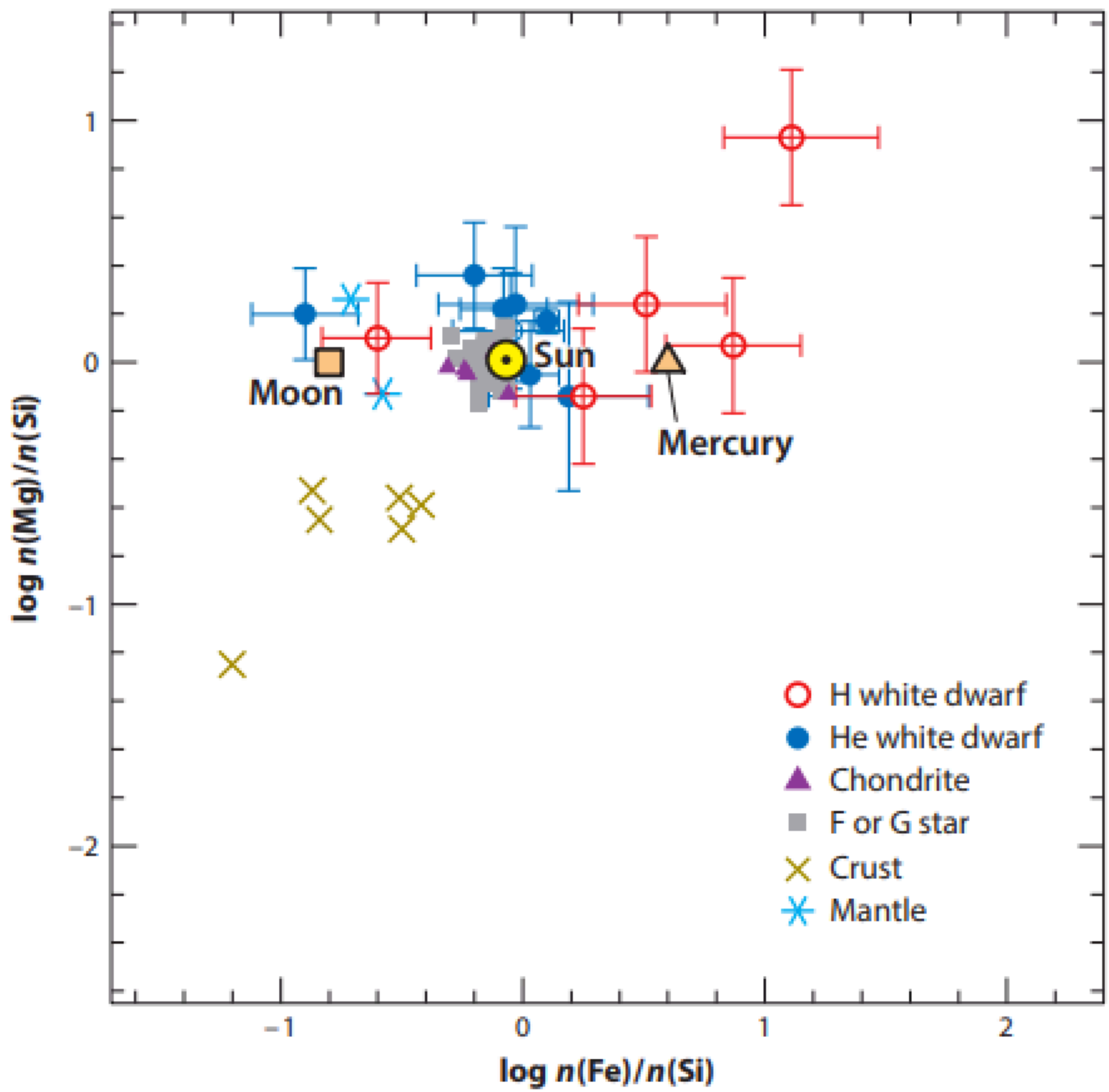

Jura & Young, 'Extrasolar cosmochemistry,' Annual Reviews, 2014

HABITABLE-ZONE 1-2 EARTH RADIUS PLANETS ARE LIKELY DIVERSE COMPOSITIONALLY

- WATER

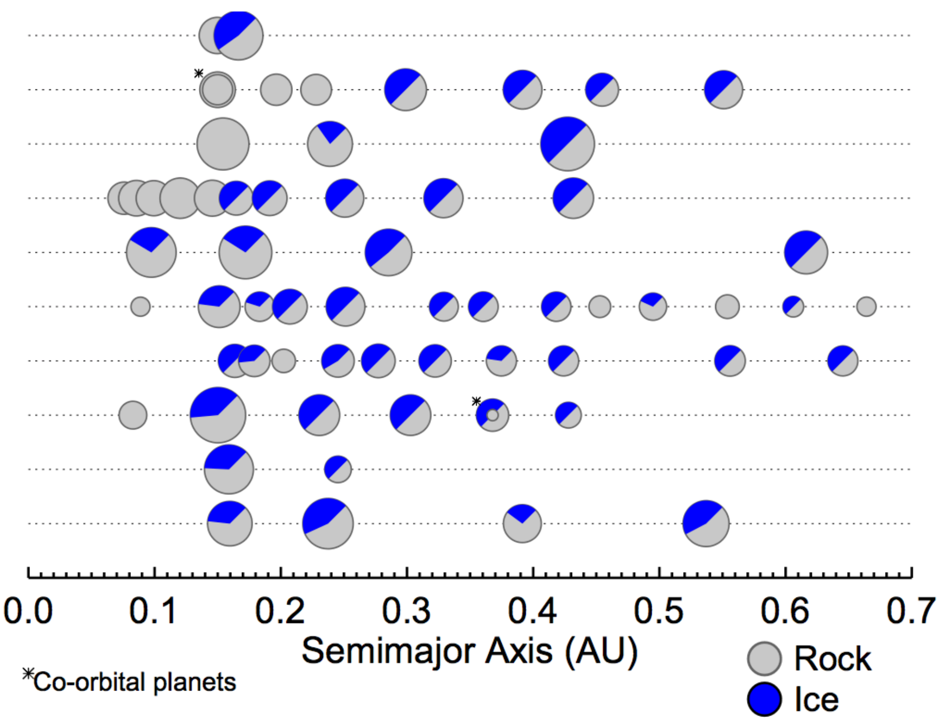

Figure 3. Final configuration of ten simulations illustrating the range of outcomes. Each planet's colors represent its rough composition: grey indicates rock and blue represents ice. Embryos that started past 5 AU started as 50-50 rock-ice mixtures and those from inside 5 AU were purely rocky. We do not account for various water loss processes and so the ice contents of simulated planets are certainly overestimates. The sizes of planets are scaled to their mass$^{1/3}$. The Kepler-36 analog system from Section 3 is at the top. Two co-orbital systems are marked with an asterisk.

Raymond et al. MNRAS Letters accepted

CYCLE-INDEPENDENT PLANETARY HABITABILITY ON EXOPLANET WATERWORLDS?

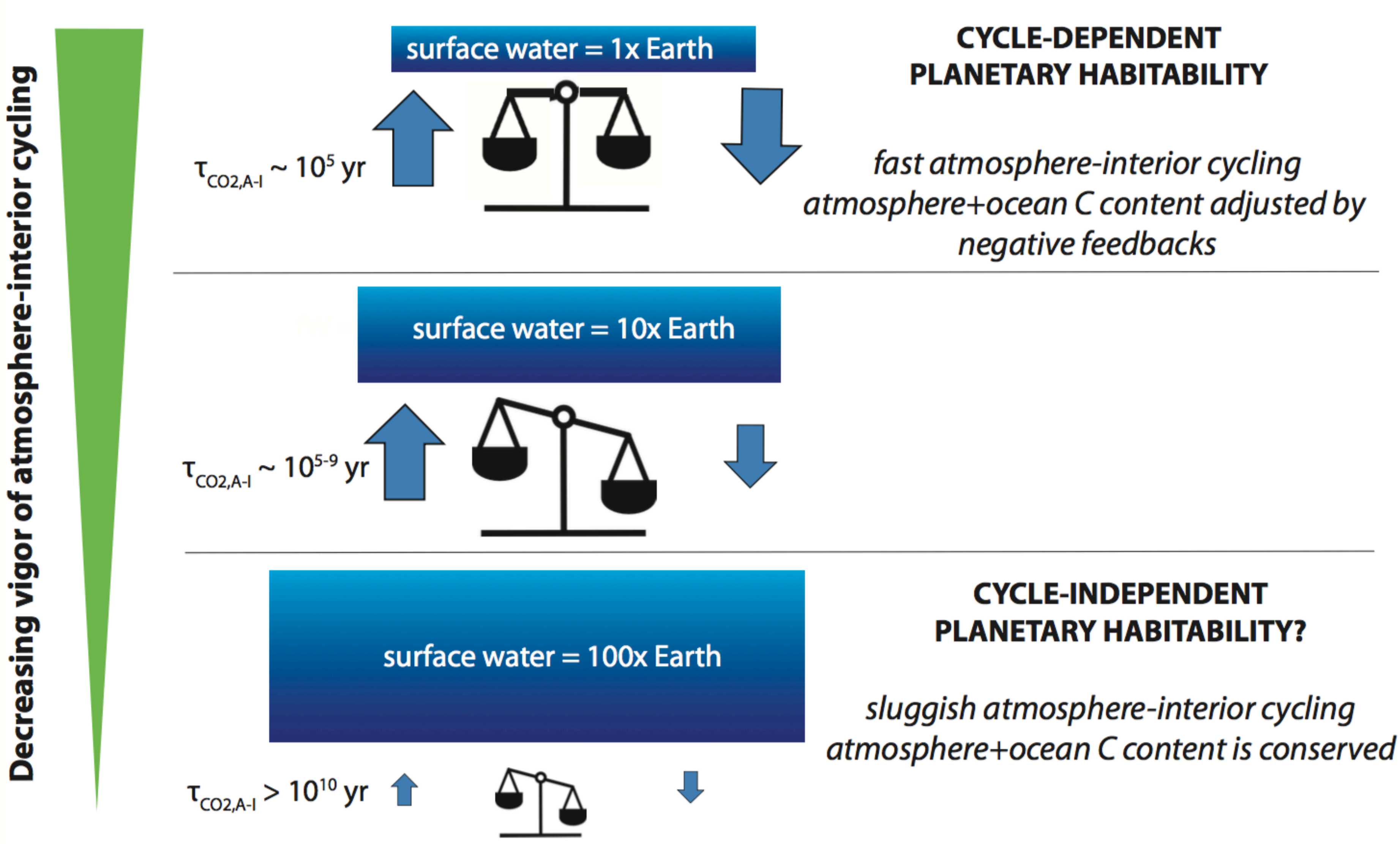

Kite & Ford, in revision

HABITABLE-ZONE 1-2 EARTH RADIUS PLANETS ARE LIKELY DIVERSE COMPOSITIONALLY

- CARBON

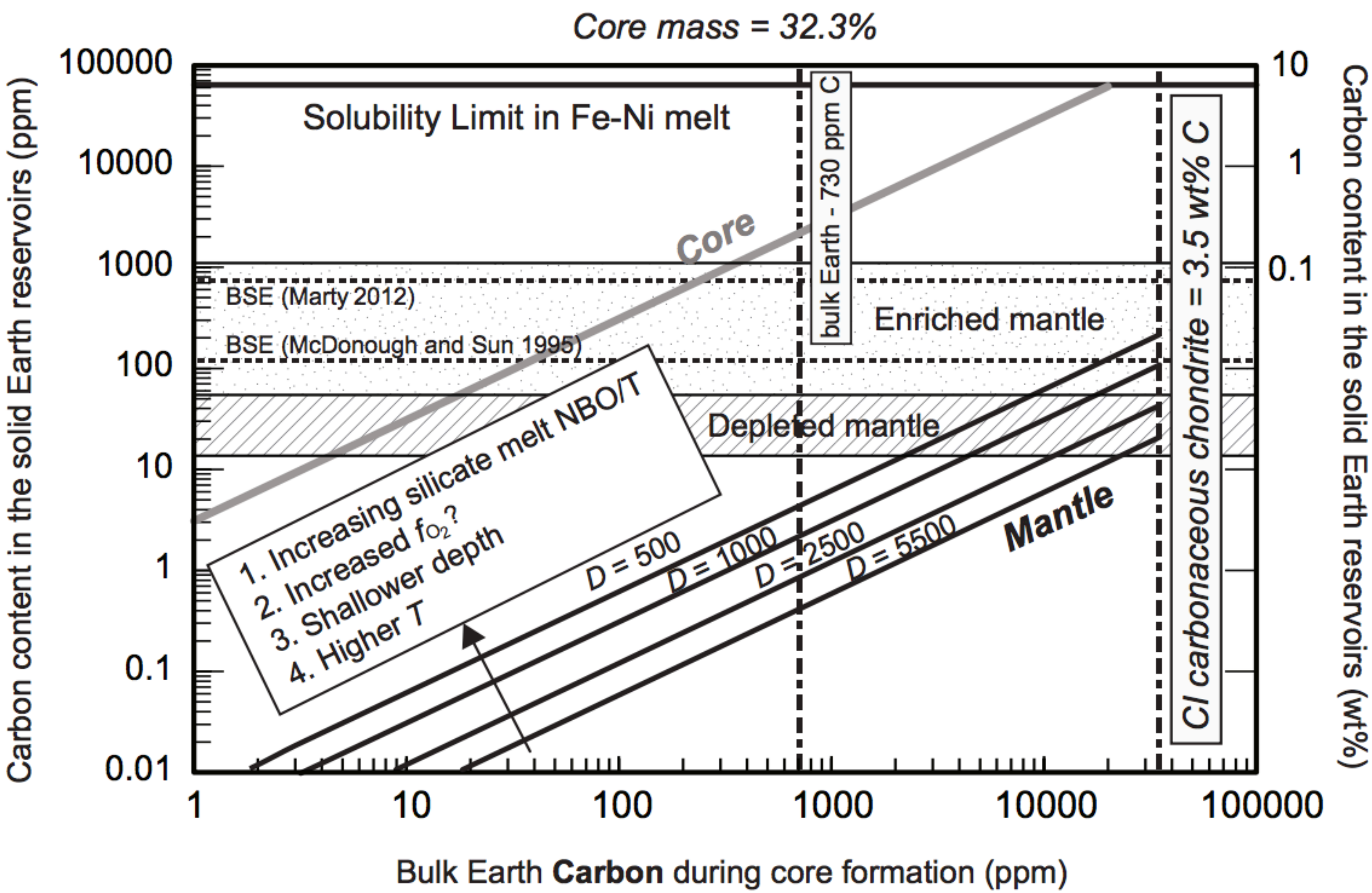

Dasgupta et al. 2013, Reviews in Mineralogy & Geochemistry

THE M-STAR OPPORTUNITY: RELATIVELY DEEPER AND MORE FREQUENT TRANSITS
→ EASIER TO DETECT & CHARACTERIZE

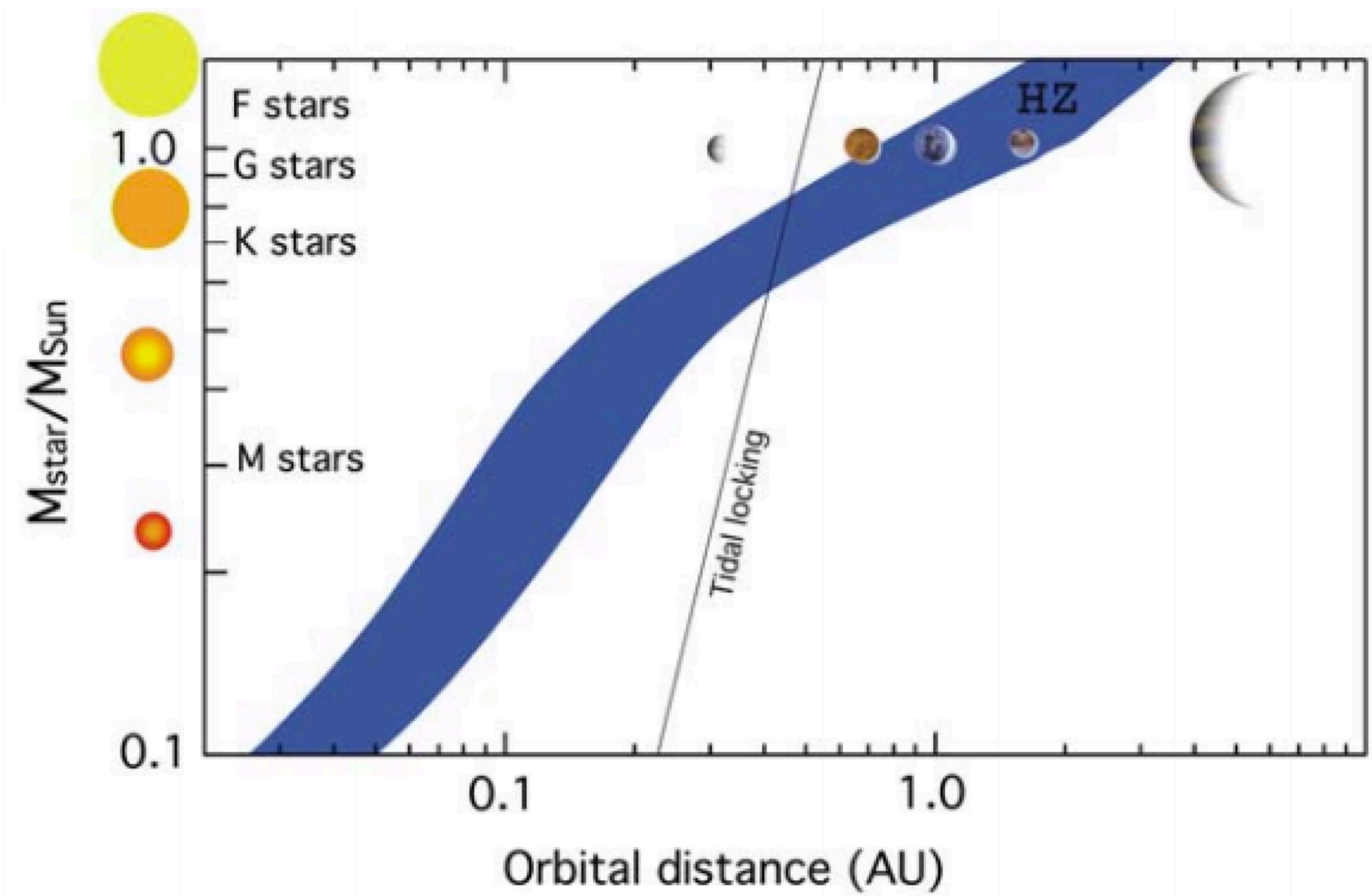

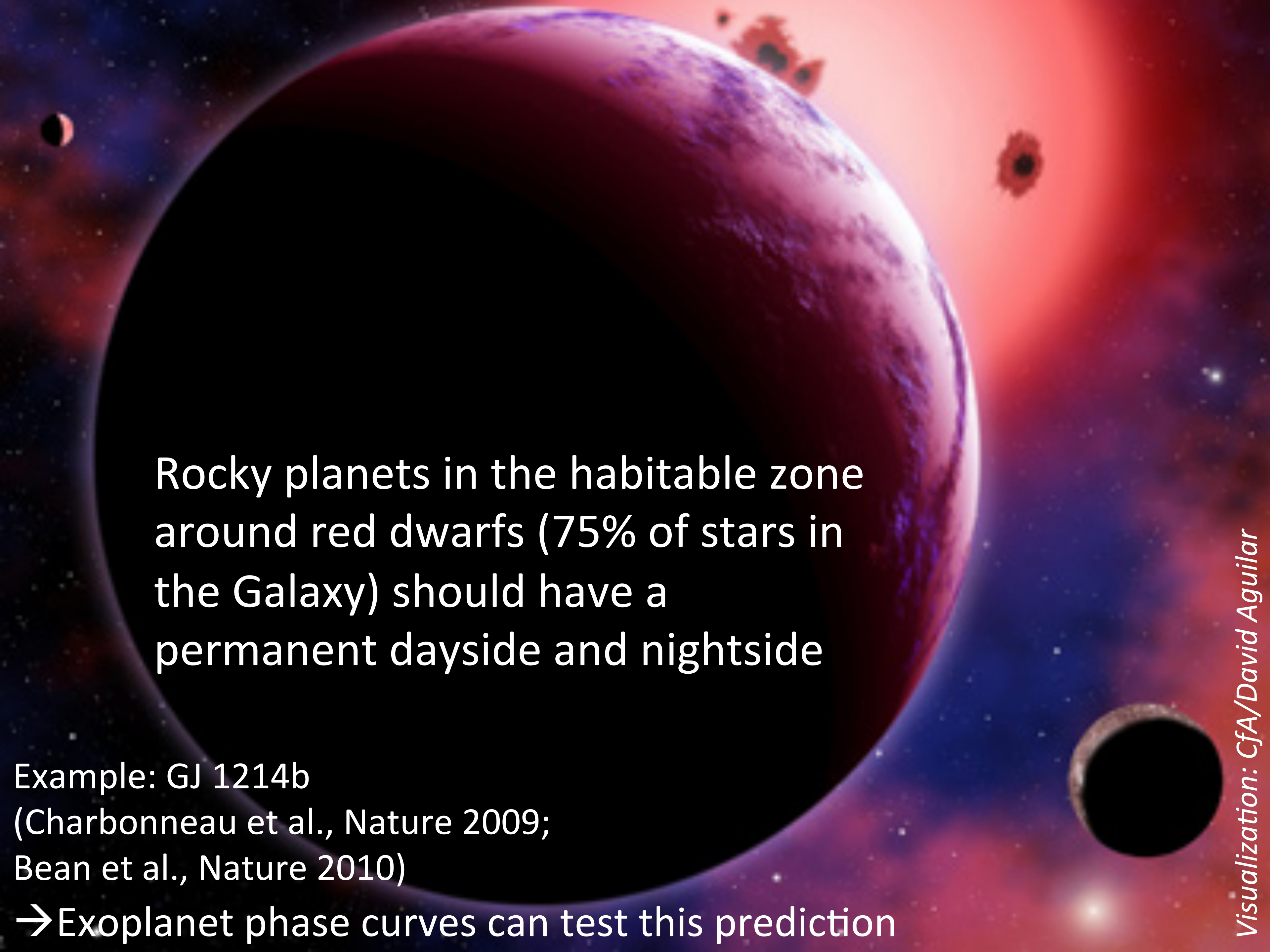

Visualization: CfA/David Aguilar

Rocky planets in the habitable zone around red dwarfs (75% of stars in the Galaxy) should have a permanent dayside and nightside

Example: GJ 1214b
(Charbonneau et al., Nature 2009;
Bean et al., Nature 2010)

→Exoplanet phase curves can test this prediction

HIGH XUV FLUX SUSTAINED FOR LONG PERIOD FOR SMALL STARS

Table 3 Time span in Gyr where $L_x/L_{bol(Sun)}$ as a function of stars with masses $\leq 1 M_{Sun}$ where the $L_x/L_{bol(Sun)}$ is about 1,700 and $\geq$ 100 times larger than at the present Sun (after Scalo et al. 2007)

M_{Sun}	t [Gyr] for 1,700 $L_x/L_{bol(Sun)}$	t [Gyr] for $\geq 100 L_x/L_{bol(Sun)}$
1.0	~0.05	~0.3
0.9	~0.1	~0.48
0.8	~0.15	~0.65
0.7	~0.2	~1.0
0.6	~0.3	~1.47
0.5	~0.5	~2.0
0.4	~0.75	~3.0
0.3	~1.0	~4.15
0.2	~1.58	~6.5
0.1	~4.6	>10.0

Lammer et al. 2009 Space Science Reviews

STRONGER STELLAR WIND → STRONGER NONTHERMAL ATMOSPHERIC ESCPAE

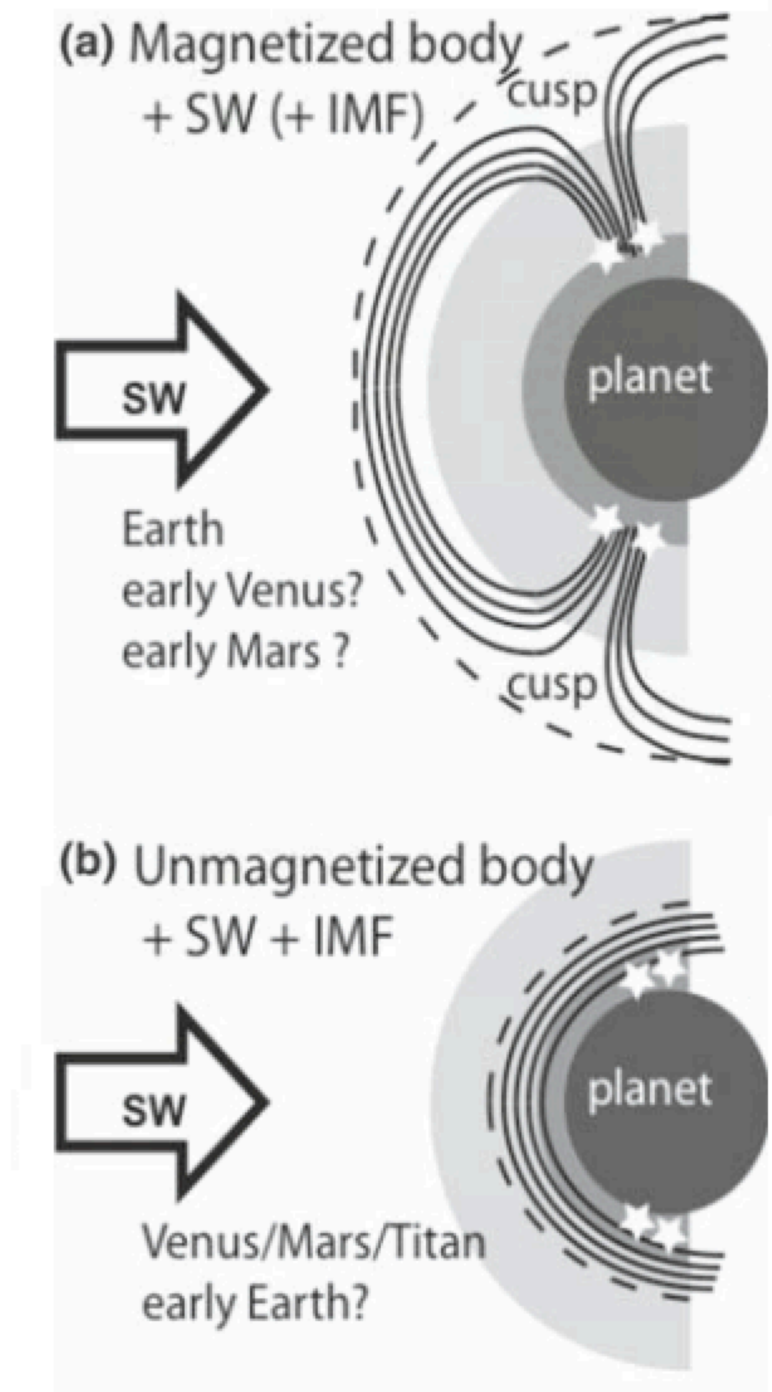

ADDITIONAL PROBLEMS FOR HABITABILITY FOR PLANETS ORBITING M-STARS

Enhanced Substellar Weathering Instability

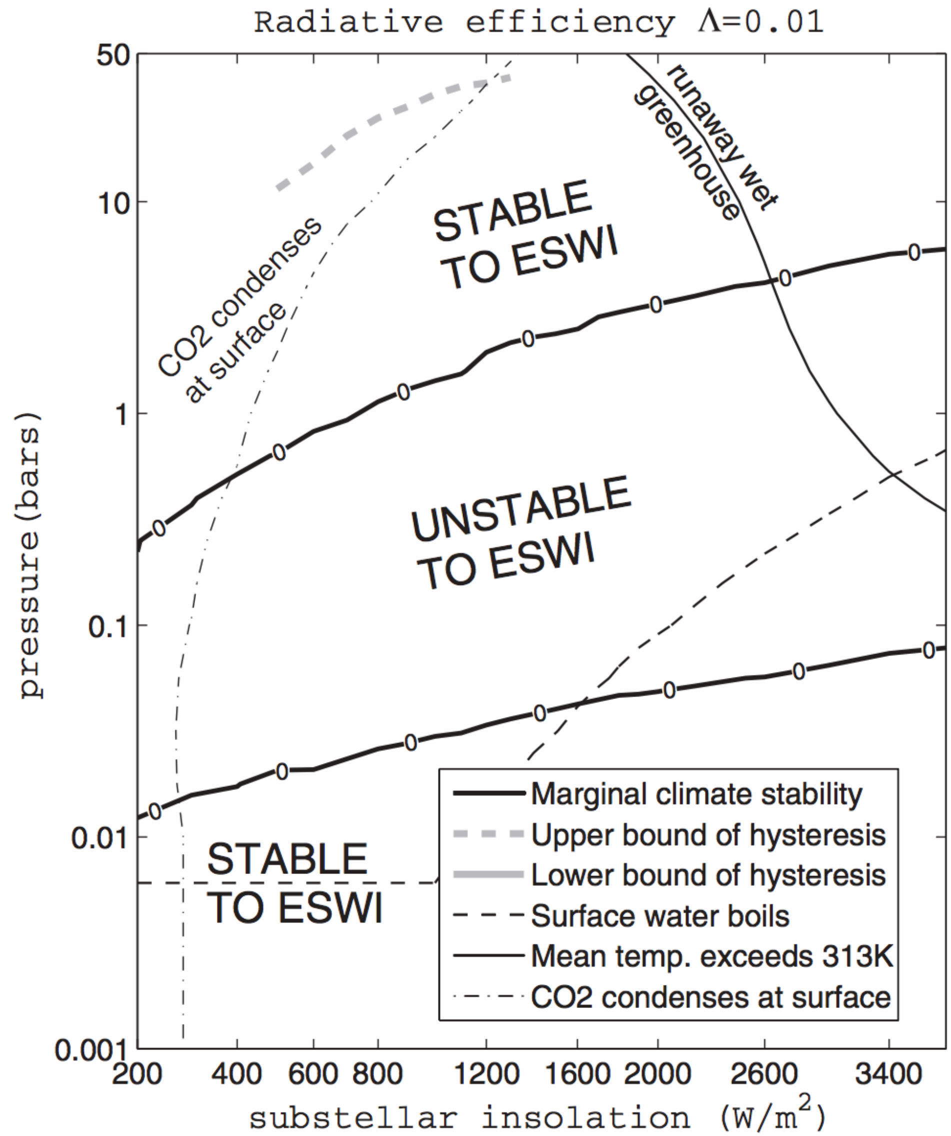

Tarter et al. Astrobiology 2007

Kite et al. ApJ 2011

INTERSTELLAR MISSIONS?

- Current distance record: Voyager 1 @ 0.8 light-days
- No interstellar missions have been funded
- The technology for an interstellar mission does not currently exist
- Breakthrough Starshot is a philanthropically-funded technology development project for a laser-accelerated interstellar lightsail

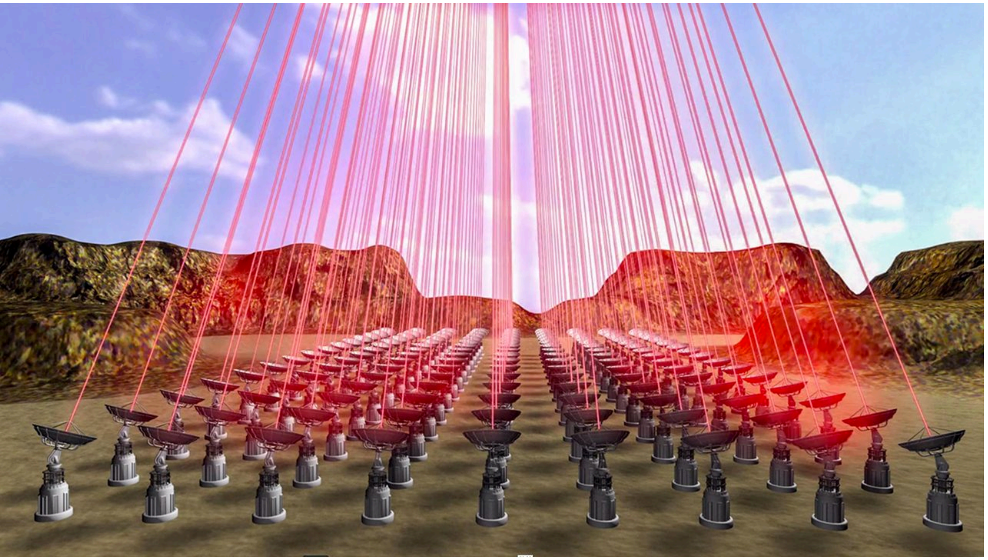

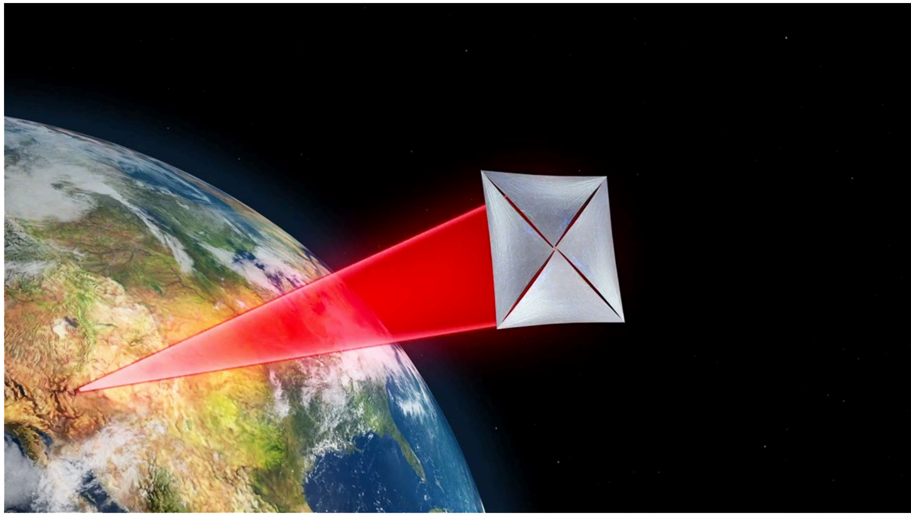

50-70GW power, 0.1 gram payload, 5000g acceleration, 0.2c cruise speed